Development 139, 3499-3509 (2012) doi:10.1242/dev.079582

Antagonistic cross-regulation between Wnt and Hedgehog signalling pathways controls post-embryonic retinal proliferation

Caroline Borday[1,*], Pauline Cabochette[1,*], Karine Parain[1], Nicolas Mazurier[1], Sylvie Janssens[2], Hong Thi Tran[2], Belaïd Sekkali[2], Odile Bronchain[1], Kris Vleminckx[2], Morgane Locker[1] and Muriel Perron[1,‡]

SUMMARY

Continuous neurogenesis in the adult nervous system requires a delicate balance between proliferation and differentiation. Although Wnt/β-catenin and Hedgehog signalling pathways are thought to share a mitogenic function in adult neural stem/progenitor cells, it remains unclear how they interact in this process. Adult amphibians produce retinal neurons from a pool of neural stem cells localised in the ciliary marginal zone (CMZ). Surprisingly, we found that perturbations of the Wnt and Hedgehog pathways result in opposite proliferative outcomes of neural stem/progenitor cells in the CMZ. Additionally, our study revealed that Wnt and Hedgehog morphogens are produced in mutually exclusive territories of the post-embryonic retina. Using genetic and pharmacological tools, we found that the Wnt and Hedgehog pathways exhibit reciprocal inhibition. Our data suggest that Sfrp-1 and Gli3 contribute to this negative cross-regulation. Altogether, our results reveal an unexpected antagonistic interplay of Wnt and Hedgehog signals that may tightly regulate the extent of neural stem/progenitor cell proliferation in the *Xenopus* retina.

KEY WORDS: Neural stem cells, Retina, Wnt and Hedgehog signalling

INTRODUCTION

Neural stem cells (NSCs) proliferate and generate new neurons throughout the lifetime in neurogenic areas of the adult brain. Identifying microenvironmental cues that tightly control their self-renewal, proliferation and lineage decisions is crucial for the development of novel therapies in regenerative medicine. Among key diffusible factors, Sonic hedgehog (Shh) is thought to be involved in adult NSC maintenance and proliferation control (Ahn and Joyner, 2005; Balordi and Fishell, 2007; Han et al., 2008; Lai et al., 2003; Machold et al., 2003; Palma et al., 2005; Po et al., 2010). The canonical Wnt pathway has also proven to be an important regulator of proliferation and neurogenesis in adult hippocampal or subventricular zones (Adachi et al., 2007; Kuwabara et al., 2009; Lie et al., 2005). Thus, both signalling pathways seem to share a mitogenic function within these neurogenic niches of the adult nervous system. However, whether the two pathways establish functional interactions in this context has not been addressed. To date, this issue has only been investigated during embryonic development. A recent study reported that these pathways cooperate in the developing spinal cord to coordinately regulate neural cell cycle progression (Alvarez-Medina et al., 2009). This clearly contrasts with the situation described in the midbrain in which Shh repression by Wnt signalling is required for floor plate neurogenesis (Joksimovic et al., 2009). Therefore, despite the vast literature on Wnt and Hedgehog mitogenic effects, the nature of their interactions is difficult to predict and clearly deserves further investigation.

Here, we have addressed this issue in the mature retina by taking advantage of the paradigmatic *Xenopus* ciliary marginal zone (CMZ), a region with active NSCs in its most peripheral region that allows continuous retinal growth during adulthood (Wetts et al., 1989; Perron et al., 1998; Cerveny et al., 2011). It was recently demonstrated that these cells in the fish retina are indeed genuine multipotent stem cells (Centanin et al., 2011). We previously showed that canonical Wnt signalling is required to maintain cell proliferation within the CMZ (Denayer et al., 2008). In addition, we found that the Hedgehog pathway has dual functions during retinogenesis, simultaneously promoting cell cycle progression as well as withdrawal of embryonic retinal progenitors (Agathocleous et al., 2007; Locker et al., 2006). Altogether, this precludes a straightforward prediction of how retinal stem/progenitor cells integrate the two signals within the CMZ. Here, we discovered that altering the two pathways leads to opposite proliferative responses. This functional antagonism correlates with non-overlapping production sites of the corresponding morphogens. We also demonstrated that Wnt and Hedgehog signalling pathways restrain each other's activity through the transcriptional regulation of *Gli3* and *Sfrp-1*. We propose a model in which the antagonistic interplay of Wnt and Hedgehog signals, emanating from opposite sides of the CMZ, controls the fine-tuning of post-embryonic proliferation in the retina.

MATERIALS AND METHODS

Embryo collection and transgenic lines

Xenopus laevis embryos were obtained by conventional methods of hormone-induced egg laying and in vitro fertilisation, and staged according to Nieuwkoop and Faber's table of development (Nieuwkoop and Faber, 1994). Transgenic *Xenopus tropicalis* carrying the Wnt reporter construct pbin8LefdGFP have been described previously (Tran et al., 2010). Briefly, the transgene, flanked by chromosomal insulator sequences, contains a synthetic promoter harbouring eight copies of an optimal binding sequence for LEF/TCF upstream of a destabilised eGFP. *X. tropicalis* transgenic embryos were obtained by natural fertilisation between a wild-type female

[1]Université Paris-Sud, UPR CNRS 3294, 91405 Orsay, France. [2]Department of Biomedical Molecular Biology, Ghent University, B-9052 Ghent, Belgium.

*These authors contributed equally to this work
‡Author for correspondence (muriel.perron@u-psud.fr)

Accepted 12 July 2012

and a transgenic male. The latter was selected beforehand as having a single transgene insertion site (as inferred by mendelian ratios in its progeny) in order to ensure homogeneous levels of GFP expression in the offspring.

Construction of the LEF1-VP16 and LEF1-EnR transgenesis vectors has been described previously (Denayer et al., 2008) and transgenic *X. tropicalis* lines (LEF1-VP16Tg and LEF1-EnRTg) were generated as described (Sekkali et al., 2008). These constructs are fused with the dexamethasone-responsive hormone-binding domain of the human glucocorticoid receptor (GR).

Expression constructs and morpholinos

pCS2-TCF3-VP16GR and *pCS2-dnTCF3-GR* (de Croze et al., 2011), *pCS2-Ihh-CD2* [previously called *Bhh* (Locker et al., 2006)], *pCS2-Smo-M2* (Koebernick et al., 2003), *pCS2-cyclinA2* and *pCS2-cdk2* (Decembrini et al., 2006) and *pCS2-GFP* (a gift from David Turner, University of Michigan, Ann Arbor, USA) were described previously. *pCS2-Shh-CD2* and *pCS2-Dhh-CD2* (previously called *Chh*) were generated by subcloning the N-terminal coding regions (devoid of the C-terminal cleavage product) of *Shh* and *Dhh* cDNAs (Ekker et al., 1995) into a *pCS2-CD2* vector (Locker et al., 2006) after PCR amplification. *Gli3* and *Sfrp-1* morpholino (Mo) sequences are shown in supplementary material Fig. S1.

Microinjection and in vivo DNA lipofection

Capped mRNAs encoding TCF3-VP16GR and GFP were transcribed from pCS2 plasmids after *Not*I digestion using the mMessage mMachine SP6 Kit (Ambion). Then, 400 pg of each mRNA was injected into two blastomeres of four-cell stage embryos. *Gli3*, *Sfrp-1* or standard control morpholino oligonucleotides (Gene Tools) were injected into one blastomere at the one-cell stage (30 ng). Their efficacy was tested by analysing in vivo GFP fluorescence following co-injection of a chimeric *GFP* construct fused downstream of the morpholino-complementary sequence (supplementary material Fig. S1).

Lipofection experiments were performed by cotransfecting the indicated *pCS2* constructs together with *pCS2-GFP* at stage 18 into the presumptive region of the retina, as previously described (Ohnuma et al., 2002). Tadpoles were fixed in 4% paraformaldehyde at stage 41 and cryostat sectioned (12 μm). GFP-positive cells were counted and cell types were identified based upon their laminar position and morphology.

Protein activity of GR chimeric constructs was induced by incubating the embryos/tadpoles for 24 hours in 4 μg/ml dexamethasone (DEX, Sigma) from stage 18 (lipofection experiments) or stage 28/30 (injection experiments, transgenic lines).

Pharmacological and recombinant SFRP-1 protein treatments

Cyclopamine (20-100 μM; LC Laboratories) or purmorphamine (100 μM; Calbiochem) was applied to the tadpole culture medium for 24 hours. BIO (6-bromoindirubin-3′-oxime, Sigma) and LiCl (Sigma) treatment conditions were adapted to tadpole stages based on the protocols of Meijer and collaborators (Meijer et al., 2003). Those for IWR-1 (Sigma) were adapted from published data on zebrafish (Chen et al., 2009). Concentrations used and drug treatment durations were: BIO, 50 μM for 1 hour; LiCl, 0.3 M for 5 minutes; IWR-1, 50 μM for 24 hours. Control tadpoles were exposed to equivalent dilutions of the corresponding drug solvent (ethanol or dimethyl sulphoxide). Recombinant chick SFRP-1 protein (R&D Systems and a gift from Paola Bovolenta) was described previously (Esteve et al., 2003). Wnt reporter transgenic tadpoles were immersed for 24 hours in 0.1× modified Barth's saline containing 3 ng/μl of the purified soluble SFRP-1 protein. Holes were made in the epidermis to facilitate the penetration of SFRP-1. For analyses at stage 41, drugs or recombinant proteins were applied 24 hours earlier, at stage 39. For analyses at stage 38 or 40 (*X. laevis* or *X. tropicalis*, respectively), they were applied at stage 28/30.

EdU/BrdU incorporation and immunohistochemistry

Tadpoles were injected intra-abdominally or immersed for 3 hours in a 10 mM BrdU solution (Sigma) and then fixed in 4% paraformaldehyde. For birthdating experiments, tadpoles were injected with 1 mM 5-ethynyl-20-deoxyuridine (EdU, Invitrogen) and subsequently incubated in a 1 mM EdU solution so that EdU would be constantly available. The solution was renewed daily. EdU incorporation was detected on paraffin sections using the Click-iT EdU Imaging Kit according to the manufacturer's protocol (Invitrogen). Immunohistochemistry was performed on 12 μm cryostat sections as described (Perron et al., 2003), with mouse monoclonal anti-BrdU (1:100, Becton Dickinson), mouse monoclonal anti-GFP (1:500, Molecular Probes), rabbit polyclonal anti-CRALBP (1:1000; an anti-glia antibody provided by Jack Saari, University of Washington, Seattle, USA), mouse monoclonal anti-XAR1 (1:10; a gift from Donald Sakaguchi, Iowa State University, Ames, USA), mouse monoclonal anti-calbindin (1:100, Swant), mouse monoclonal anti-Islet1 (1:100, DSHB), and anti-mouse or anti-rabbit fluorescent secondary antibodies (1:1000, Alexa 488 or 594, Molecular Probes). Mouse monoclonal anti-PCNA (1:1000, Dako) was applied on 12 μm paraffin sections from tadpoles fixed in Bouin solution. Cell nuclei were counterstained with Hoechst (Sigma). Fluorescent staining was visualised with a Zeiss M2 microscope. Images were captured using an AxiocamMRc digital camera (Zeiss) and processed with AxioVision REL 7.8 (Zeiss) and Photoshop CS4 (Adobe) software.

In situ hybridisation

Digoxigenin-labelled antisense RNA probes were generated according to the manufacturer's instructions (DIG RNA Labeling Mix, Roche). Whole-mount in situ hybridisation was carried out as previously described (Perron et al., 2003). Embryos were then vibratome sectioned (50 μm).

Quantitative real-time PCR (qPCR)

Total RNA from 40-100 dissected retinas was isolated using the Aurum Total RNA Fatty and Fibrous Tissue Kit (BioRad) or the Nucleospin RNA XS Kit (Macherey Nagel). Reverse transcription was performed using the iScript cDNA Synthesis Kit (BioRad). qPCR reactions were performed in triplicate using SsoFast EvaGreen Supermix (BioRad) on a C1000 thermal cycler (CFX96 real-time system, BioRad). Results were normalised against the expression of reference genes *ODC* and *RPL8* using CFX Manager software (BioRad). PCR primer sequences are listed in supplementary material Table S1.

Quantification and statistical analyses

At least six embryos per condition and per experiment were analysed. Following image capture, areas of the in situ hybridisation labelling in the CMZ were quantified using AxioVision REL 7.8 or Photoshop CS4. As the signal in the control condition can vary along the dorsoventral axis, quantification was systematically performed in both the dorsal and ventral CMZ. Numeration of BrdU-positive cells in the CMZ was performed by manual counting following delineation of the dorsal and ventral CMZ based on Hoechst staining. Changes in BrdU-positive cell number are presented as percentage increase/decrease relative to the average number found in control CMZ. Statistical analysis was performed using Student's *t*-test ($P \leq 0.05$).

RESULTS

Hedgehog and Wnt pathways lead to opposite proliferative phenotypes during retinogenesis

As a first step to compare Wnt and Hedgehog involvement in retinal stem/progenitor cell behaviour, we activated each pathway during retinogenesis by in vivo lipofection and performed lineage analyses of transfected cells in the mature retina (Fig. 1, supplementary material Fig. S2). Canonical Wnt signalling activation was achieved by overexpressing a constitutively active form of TCF3 (TCF3-VP16GR) (Agathocleous et al., 2009), a transcriptional effector acting at the nuclear endpoint of the pathway. As previously shown (Agathocleous et al., 2009), forced *TCF3* expression in such assays leads to the maintenance of cells retaining a neuroepithelial morphology characteristic of retinal progenitors (Fig. 1A,C). Agathocleous and collaborators further demonstrated that these neuroepithelial cells are actively proliferating, consistent with a Wnt-induced delay in cell cycle

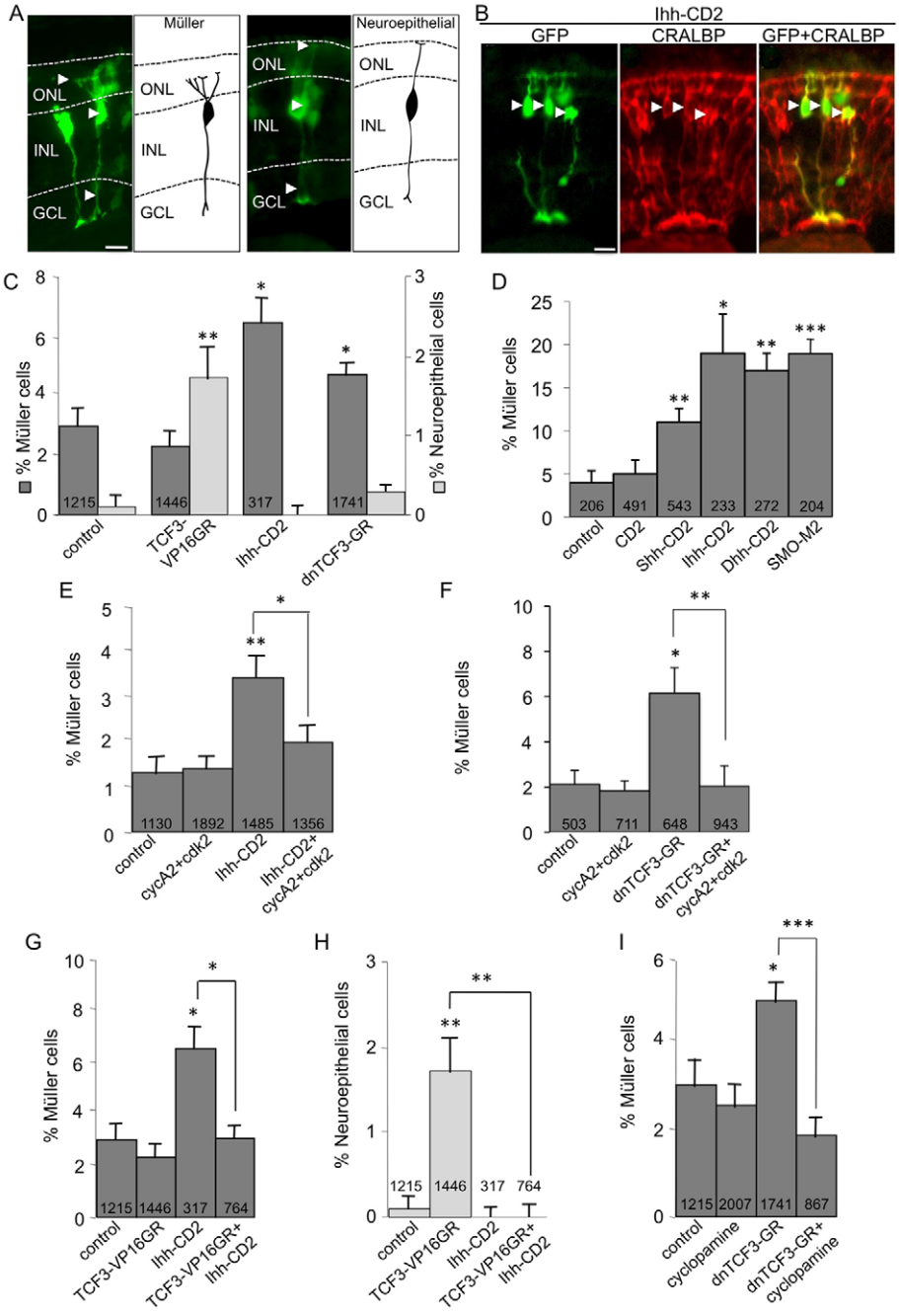

Fig. 1. Interfering with Hedgehog and Wnt pathways leads to opposite effects on precursor cell destiny during retinogenesis. (**A**,**B**) Stage 41 *Xenopus* retinal sections following in vivo lipofection. (A) The respective morphologies of GFP-positive Müller versus neuroepithelial cells. Arrowheads indicate the cell represented in the adjacent drawing. (B) Anti-CRALBP immunostaining (Müller cell marker; arrowheads) following Ihh-CD2 overexpression. (**C-I**) Percentage of Müller or neuroepithelial cells observed in stage 41 retinas following in vivo lipofection with the indicated constructs. Cyclopamine treatment was performed from stage 18 onwards on embryos lipofected with *GFP*. The total number of counted cells per condition is indicated in each bar. **P*<0.05, ***P*<0.01, ****P*<0.001 (Student's *t*-test). Mean ± s.e.m. ONL, outer nuclear layer; INL, inner nuclear layer; GCL, ganglion cell layer. Scale bars: 10 μm.

withdrawal (Agathocleous et al., 2009). We then lipofected *Ihh-CD2*, a construct that encodes a membrane-anchored Indian hedgehog (Ihh) protein, allowing for cell-autonomous activation of Hedgehog signalling (Locker et al., 2006). In contrast to the previous situation, *Ihh-CD2* overexpression did not enhance the proportion of neuroepithelial cells but instead induced a 3-fold increase in Müller glia (Fig. 1A,C), as confirmed by immunostaining using an anti-CRALBP antibody (Fig. 1B). A similar increase in the proportion of Müller cells was obtained upon misexpression of the two other Hedgehog ligands [Shh and Desert hedgehog (Dhh)] and of a constitutively active form of Smoothened called Smo-M2 (Fig. 1D).

Intriguingly, studies in *Xenopus* have revealed that overexpression of cyclin-dependent kinase inhibitors of the Cip/Kip (Ohnuma et al., 1999; Daniels et al., 2004) or INK (M. Agathocleous and M. Roussel, personal communication) families both pushes precursors out of the cell cycle and favours Müller cell genesis. In line with this, could the Hedgehog-dependent bias toward gliogenesis be linked in any way to the previously demonstrated ability of the pathway to promote precocious cell cycle exit (Locker et al., 2006)? We addressed this issue by counteracting *Ihh*-induced effects on cell cycle withdrawal through co-lipofection with *cyclinA2*/*cdk2*. These two cell cycle components are known, when co-overexpressed, to delay retinal cell birthdate without altering cell cycle kinetics (Decembrini et al., 2006). We indeed found that this rescued the Müller glia phenotype (Fig. 1E), leading to a retinal cell distribution indistinguishable from that observed in controls (supplementary material Fig. S3A). Importantly, the same held true following blockade of Wnt signalling: overexpression of a dominant-negative form of TCF3

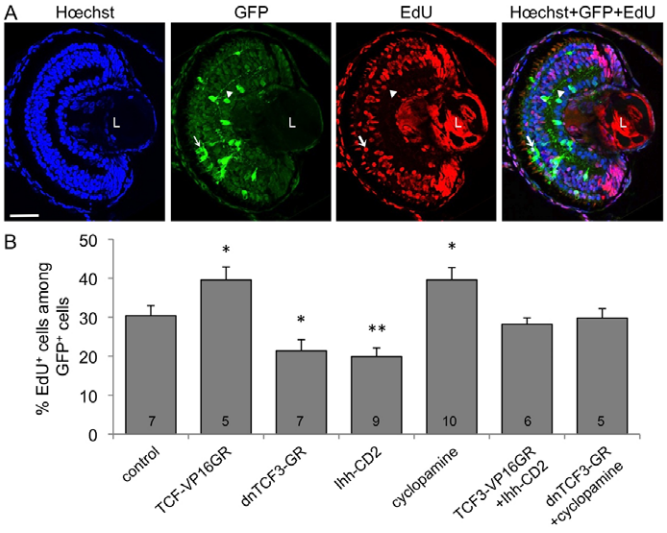

Fig. 2. Hedgehog and Wnt pathways have opposite impacts on cell cycle exit. Birthdating experiments (from stage 32 to stage 41) following in vivo lipofection with the indicated constructs. Cyclopamine treatment was performed from stage 18 onwards on embryos lipofected with *GFP*. Transfected cells that have exited the cell cycle before EdU exposure (stage 32) are EdU$^-$ at stage 41, whereas cells that have exited the cell cycle at any time during the EdU incorporation period are EdU$^+$. (**A**) Typical stage 41 retinal sections stained for GFP and EdU. The arrow and arrowhead point to a GFP$^+$ EdU$^+$ and to a GFP$^+$ EdU$^-$ cell, respectively. (**B**) Percentage of EdU$^+$ nuclei among transfected cells. The total number of analysed retinas per condition is indicated in each bar. *P<0.05, **P<0.01 (Student's t-test). Mean ± s.e.m. L, lens. Scale bar: 40 μm.

(*dnTCF3-GR*) enhanced Müller cell genesis as previously shown with other constructs (Van Raay et al., 2005), and this effect was abolished upon co-lipofection with *cyclinA2*/*cdk2* (Fig. 1C,F, supplementary material Fig. S3B). We thus propose that the increased glial cell proportion induced by Hedgehog activation or Wnt inhibition results, at least in part, from precocious cell cycle exit.

We next examined whether Wnt signalling activation would be sufficient to rescue the Hedgehog phenotype, and vice versa. *TCF3-VP16GR* overexpression indeed prevented Hedgehog-dependent excess in gliogenesis (Fig. 1G). Conversely, the Wnt-induced increase in neuroepithelial cells was abolished upon *Ihh-CD2* co-lipofection (Fig. 1H). In addition, blocking Hedgehog signalling using the Smoothened antagonist cyclopamine also rescued the Müller phenotype of *dnTCF3-GR*-lipofected embryos (Fig. 1I). Together, these data show that Hedgehog and Wnt signalling pathways have opposite outcomes for retinal progenitor destiny, which is likely to reflect their inverse roles in cell cycle exit regulation. We further tested this hypothesis by directly evaluating the timing of cell cycle exit in each condition through birthdating experiments (Fig. 2). Embryos were subjected to constant EdU exposure from stage 32 to stage 41, so that all cells born in that period would be labelled. As expected, *Ihh-CD2* or *dnTCF3-GR* lipofection led to a decreased proportion of EdU-positive cells among transfected cells (including among Müller cells; supplementary material Fig. S4), showing a precocious cell cycle exit, whereas *TCF3-VP16GR* lipofection or cyclopamine treatment led to the opposite effect, indicative of a delayed cell birthdate. Finally, co-activation or co-inhibition of both pathways rescued the phenotypes back to a control situation. These data thus confirm that the Hedgehog and Wnt signalling pathways have opposite impacts on the timing of retinal cell cycle exit.

Wnt and Hedgehog pathways lead to opposite proliferative phenotypes in the post-embryonic retina

Could such a functional antagonism also hold true in the context of post-embryonic retinal neurogenesis? As a prerequisite to answering this question, we first set up experimental conditions that allow conditional Wnt and Hedgehog signalling activation or inhibition through pharmacological means. The compound 6-bromoindirubin-3′-oxime (BIO), a selective GSK-3 inhibitor (Meijer et al., 2003), and IWR-1, a small molecule that prevents Axin protein degradation (Chen et al., 2009), were previously described as an effective activator and inhibitor of the canonical Wnt pathway, respectively. We took advantage of a *X. tropicalis* Wnt reporter line (Tran et al., 2010) to control their effectiveness and determine optimal concentrations and exposure conditions. As previously described in *X. laevis* (Denayer et al., 2008), we detected Wnt activity within the CMZ (Fig. 3A). In addition, the destabilised character of the eGFP reporter allowed us to more sharply delineate the territory concerned, which appeared restricted to the peripheral half of the CMZ that includes the stem cell-containing zone. This territory was found to be significantly expanded 24 hours following BIO treatment and dramatically reduced upon IWR-1 exposure (Fig. 3B,C). We thus used these conditions for subsequent analyses. Activity of Hedgehog signalling was assessed through the expression of its target genes *Patched-1* (*Ptc1*) and *Gli1* and could be detected, as expected, within the CMZ (Perron et al., 2003), as well as in the periocular mesenchyme as previously described in mouse (Dakubo et al., 2008) (Fig. 3D,E). Functional interference with the pathway was achieved using the Smoothened agonist purmorphamine and the antagonist cyclopamine. We found that a 24-hour treatment with these drugs was sufficient for consistent activation or inhibition of the pathway, respectively, as revealed by the dramatic increase or reduction of both *Ptc1* and *Gli1* staining (Fig. 3D-G).

In order to address the respective and interactive contributions of the Wnt and Hedgehog pathways to post-embryonic proliferation, we next performed BrdU incorporation assays following their pharmacological perturbation for 24 hours (Fig. 4). In this time window, although the size of the whole CMZ (as measured by the extent of the *Rx1* labelling area; supplementary material Fig. S5A,B) was seemingly unaffected, significant variations in the number of BrdU-positive cells could be detected. We previously demonstrated that Wnt signalling is required for the maintenance of proliferation at post-embryonic stages (Denayer et al., 2008). Accordingly, BIO-treated tadpoles exhibited an increased number of BrdU-labelled cells in the CMZ compared with control retinas, whereas proliferation levels significantly dropped following IWR-1 treatment (Fig. 4B). Strikingly, exposure to purmorphamine reduced BrdU incorporation below the control level, as observed for IWR-1 treatment. Conversely, tadpole exposure to cyclopamine increased BrdU-positive cell number within the CMZ, thus phenocopying the BIO treatment (Fig. 4B). Moreover, similar changes in the number of PCNA-positive cells were observed for each condition (supplementary material Fig. S6), confirming variations in the size of the whole proliferative cell cohort. Based on our above lipofection data (Fig. 1), we reasoned that co-activating or co-inhibiting both pathways should restore a

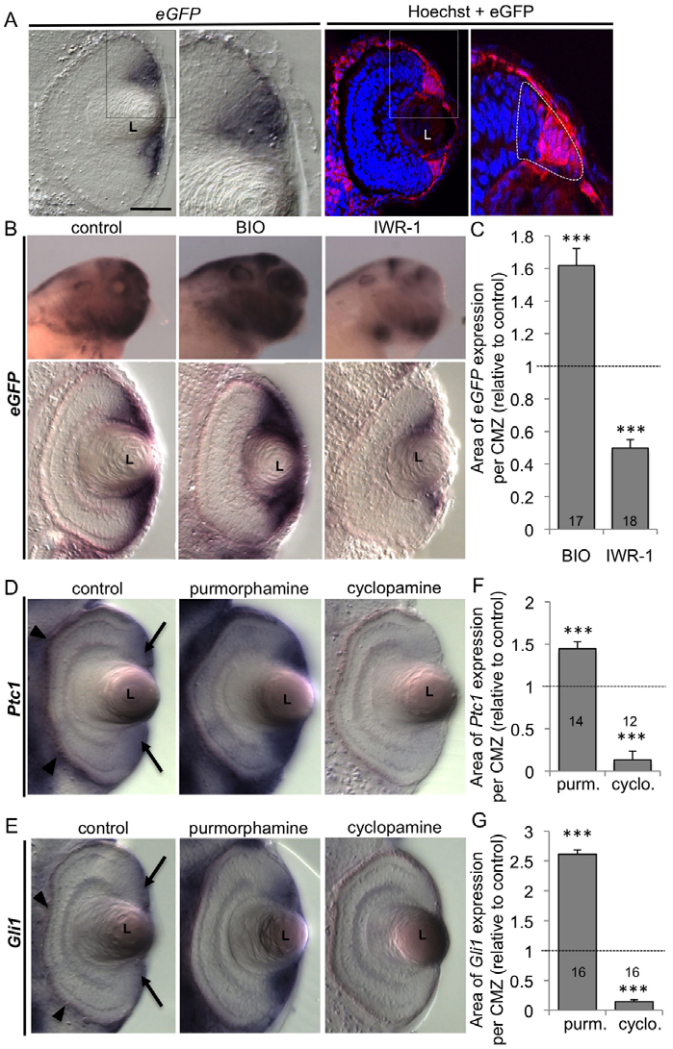

Fig. 3. BIO, IWR-1, purmorphamine and cyclopamine act as efficient Wnt and Hedgehog pathway activators or inhibitors in the *Xenopus* tadpole retina. (**A**) In situ hybridisation or immunofluorescence analyses of *eGFP* expression on stage 40 retinal sections from Wnt-responsive transgenic animals. Enlargements of the ciliary marginal zone (CMZ) region (delineated with dotted line) show that *GFP* expression is strongest in the peripheral half of the CMZ, including the stem cell zone. Note that Wnt activity is also detected in the peripheral retinal pigment epithelium (RPE). (**B**,**C**) In situ hybridisation against *eGFP* on stage 40 transgenic tadpoles 24 hours following BIO or IWR-1 treatment. (B) Representative images of staining in whole mount (lateral view of the head) and on retinal sections (dorsal side up). (C) Quantification of *eGFP* staining area per CMZ. (**D-G**) In situ hybridisation analyses of *Ptc1* (D) and *Gli1* (E) expression on stage 40 retinal sections 24 hours following purmorphamine or cyclopamine treatment. Note that *Ptc1* and *Gli1* are detected in the CMZ (arrows) and in the periocular mesenchyme (arrowheads). (F,G) Quantification of *Ptc1* and *Gli1* staining area per CMZ. The total number of analysed sections per condition is indicated in each bar. ***P<0.001 (Student's t-test). Mean ± s.e.m. L, lens. Scale bar: 40 μm, except 400 μm in whole mounts.

wild-type phenotype. Indeed, CMZ proliferation levels following BIO/purmorphamine or IWR-1/cyclopamine co-treatments were not significantly different from the control situation (Fig. 4B). These data clearly demonstrate that altering the Wnt and Hedgehog signalling pathways during a period of 24 hours leads to opposite and counterbalancing proliferative outcomes in the post-embryonic CMZ.

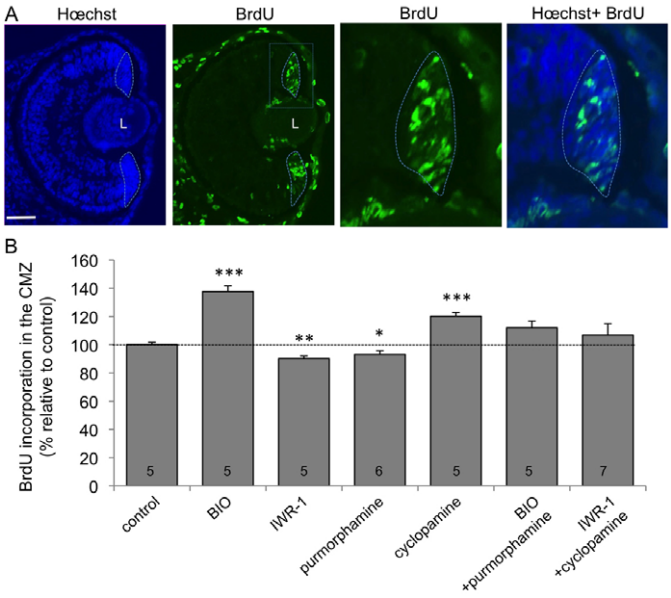

Fig. 4. Interfering with Hedgehog and Wnt pathways leads to opposite proliferative outcomes in the post-embryonic retina. BrdU incorporation assays (3-hour pulse) at stage 41, 24 hours following treatment with the indicated drugs. (**A**) Control retinal section illustrating how the CMZ, in which BrdU$^+$ cells are counted, is delineated (dotted lines) using Hoechst staining. Images on the right show higher magnifications of the CMZ. (**B**) Quantification of BrdU$^+$ cells in the CMZ. The total number of analysed retinas per condition is indicated in each bar. *P<0.05, **P<0.01, ***P<0.001 (Student's t-test). Mean ± s.e.m. L, lens. Scale bar: 40 μm.

Wnt and Hedgehog morphogens emanate from mutually exclusive territories of the post-embryonic retina

Such a negative Wnt/Hedgehog interplay is reminiscent of their well-established antagonistic functions in the patterning of the spinal cord, where they act as opposed morphogenetic signals along the dorsoventral axis (reviewed by Ulloa and Marti, 2010). We thus wondered whether such morphogen gradients could similarly take place in the CMZ, where both pathways are active (Fig. 3 and Fig. 5C). We determined the spatial distribution of Wnt and Hedgehog ligand transcripts in the mature retina by in situ hybridisation (Fig. 5 and see schematic in Fig. 10A). As previously shown (Perron et al., 2003), *Shh* is mainly expressed in the ganglion cell layer, whereas *Ihh* and *Dhh* are restricted to the central retinal pigment epithelium (RPE) and are excluded from its peripheral part surrounding the CMZ (Fig. 5A). Among Wnt ligands, neither *Wnt1*, *Wnt8*, *Wnt10b* nor *Wnt11r* could be detected in the mature retina (data not shown). Strikingly, however, *Wnt2b*, *Wnt3a*, *Wnt7b*, *Wnt8b*, *Wnt9a*, *Wnt9b* and *Wnt16* mRNAs were all localised within or around the CMZ. Labelling was found either in the peripheral RPE lining the CMZ, in the stem cell-containing zone of the CMZ, in the presumptive cornea or in epithelial cells of the lens (Fig. 5B; data not shown). Wnt and Hedgehog ligand genes thus exhibit mutually exclusive expression patterns along the central to peripheral axis of the post-embryonic retina, suggesting that opposing gradients might exist within the CMZ.

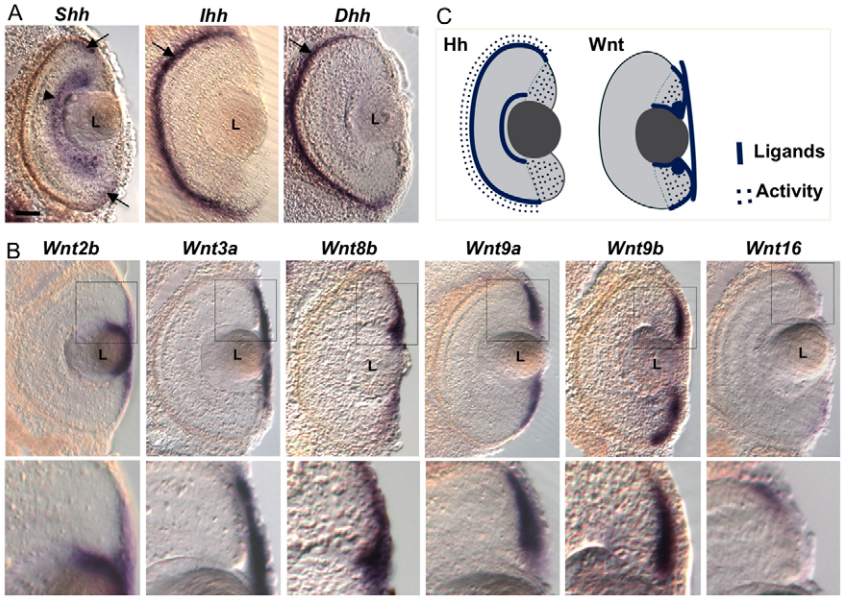

Fig. 5. Wnt and Hedgehog morphogens are expressed in mutually exclusive territories within the post-embryonic retina. (**A**,**B**) Retinal sections of stage 39/40 *Xenopus* tadpoles following in situ hybridisation with the indicated probes. (A) *Shh*, *Ihh* and *Dhh* are detected in the central RPE (arrows). Additionally, *Shh* labels the ganglion cell layer (arrowhead). (B) In contrast to Hedgehog genes, those encoding Wnt ligands are all expressed in the peripheral retina. Shown beneath each retinal section is a higher magnification of the CMZ region (boxed). *Wnt2b*, *Wnt8b*, *Wnt9a*, *Wnt9b* and *Wnt16* are detected in the peripheral RPE surrounding the CMZ (*Wnt8b* and *Wnt9a* exhibit a more intense staining dorsally than ventrally). *Wnt8b* is additionally expressed in the most peripheral stem cell-containing region of the CMZ, together with *Wnt2b*, which also labels the peripheral part of the lens. *Wnt3a* transcripts are present in the presumptive cornea and *Wnt7b* is expressed in the lens (not shown). (**C**) Summary of Hedgehog (Hh) and Wnt ligand expression in the retina, and of domains exhibiting Wnt (in the CMZ) and Hedgehog (in the CMZ and periocular mesenchyme) activity. L, lens. Scale bar: 40 μm.

The Wnt pathway restrains Hedgehog activity in the CMZ

We next investigated potential cross-regulation between the Wnt and Hedgehog cascades. Using pharmacological and genetic tools, we first analysed the impact of Wnt pathway activation on Hedgehog signalling activity by examining the effects of a 24-hour BIO treatment. Although treated retinas appeared slightly smaller than controls, no developmental delay or defects in the central retina were observed, as assessed by the normal expression pattern of various differentiated cell markers (supplementary material Fig. S7). Consistent with an effective activation of canonical Wnt signalling in the CMZ (Denayer et al., 2008), the expression of *CyclinD1*, an established Wnt transcriptional target gene, was dramatically enhanced compared with the control situation (Fig. 6A). Of note, the overall size of the CMZ as inferred from the *Rx* expression domain was not significantly affected (supplementary material Fig. S5C,D). By contrast, the expression of the Hedgehog transcriptional targets *Ptc1* and *Gli1* was virtually abolished, reflecting a significant inhibition of the pathway (Fig. 6A,B). Importantly, these results were validated by two additional strategies: *TCF3-VP16GR* overexpression by mRNA microinjection at the four-cell stage (Fig. 6C,D) and treatment with LiCl (supplementary material Fig. S8), which is the most frequently used GSK-3β inhibitor, although supposedly less specific than BIO (Meijer et al., 2003). These data suggest that activating the Wnt pathway attenuates Hedgehog signalling activity in the post-embryonic retina.

We next monitored Hedgehog activity following inhibition of Wnt signalling. Retinas of IWR-1-treated tadpoles displayed reduced *CyclinD1* staining with respect to controls. By contrast, *Gli1* and *Ptc1* expression was strongly enhanced within the CMZ (Fig. 6E,F), suggesting an increase in Hedgehog pathway activity.

To support these in situ hybridisation results, we quantified *Ptc1* expression by qPCR following genetic or pharmacological modulation of Wnt signalling. Consistent with the previous data, we found decreased *Ptc1* mRNA levels upon BIO treatment or *TCF3-VP16GR* injection and the opposite result in IWR-1-treated retinas (Fig. 6G). Finally, we confirmed these results in two *Xenopus* transgenic lines in which the Wnt pathway can be conditionally activated (LEF1-VP16 Tg) or repressed (LEF1-EnR Tg) (Fig. 6H). Together, these data suggest that the Wnt pathway is required to limit Hedgehog activity in the CMZ.

Hedgehog signalling negatively regulates Wnt activity in the CMZ

We then examined whether the Hedgehog pathway might reciprocally inhibit Wnt signalling activity. The Wnt-responsive transgenic tadpoles described above (Fig. 3) were treated for 24 hours with cyclopamine or purmorphamine and then subjected to immunofluorescence and in situ hybridisation to evaluate eGFP protein and mRNA expression levels, respectively. Hedgehog inhibition resulted in increased eGFP staining in the CMZ, whereas its activation led to the opposite phenotype (Fig. 7). Thus, Hedgehog signalling restricts Wnt activity, possibly contributing to its confinement to the peripheral part of the CMZ.

The Hedgehog pathway restricts Wnt activity in the CMZ through transcriptional regulation of *Sfrp-1*

We next investigated the molecular mechanism by which the Hedgehog and Wnt pathways establish these reciprocal cross-regulations. The gene encoding the secreted protein SFRP-1, which is an antagonist of Wnt signalling (Xu et al., 1998),

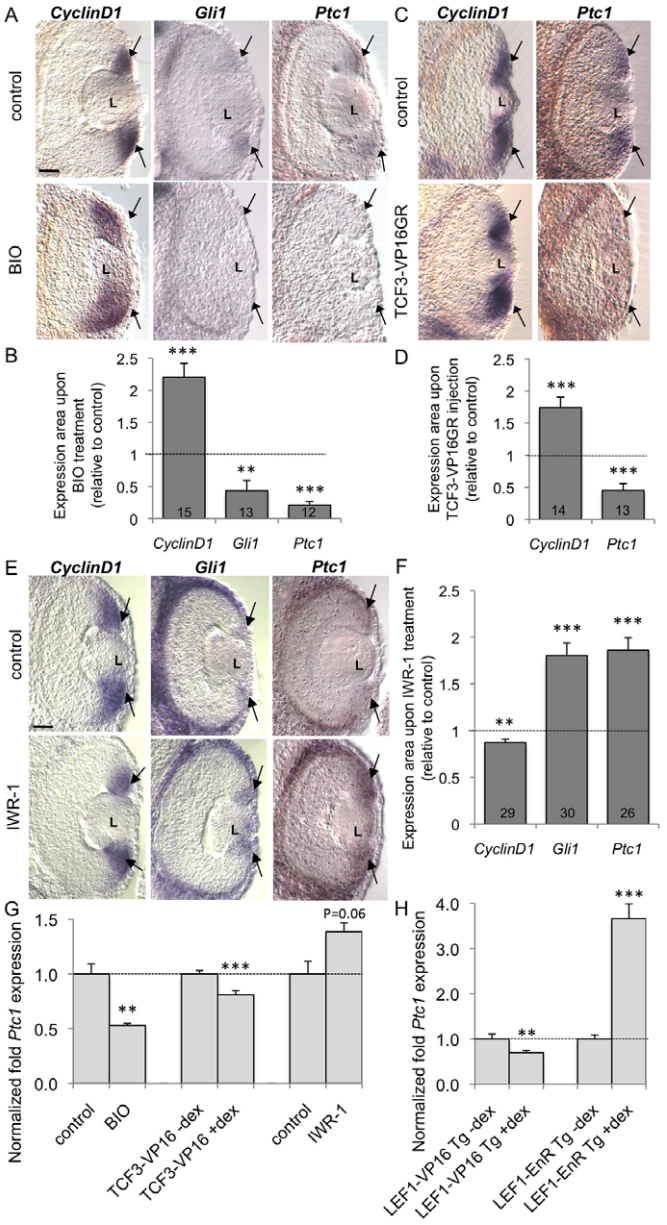

Fig. 6. Impact of Wnt pathway perturbations on Hedgehog signalling activity. (**A-F**) In situ hybridisation analyses of *CyclinD1*, *Gli1* or *Ptc1* expression on stage 38 retinal sections 24 hours following treatment with BIO (A,B), induction of TCF3-VP16GR activity in injected embryos (C,D), or treatment with IWR-1 (E,F). Arrows indicate CMZ labelling. (B,D,F) Quantifications of staining area for each transcript. The total number of analysed sections per condition is indicated in each bar. (**G**,**H**) qPCR analysis of retinal *Ptc1* expression following Wnt signalling activation or inhibition as indicated. ***P*<0.01, ****P*<0.001 (Student's *t*-test). Mean ± s.e.m. L, lens. Scale bars: 40 µm.

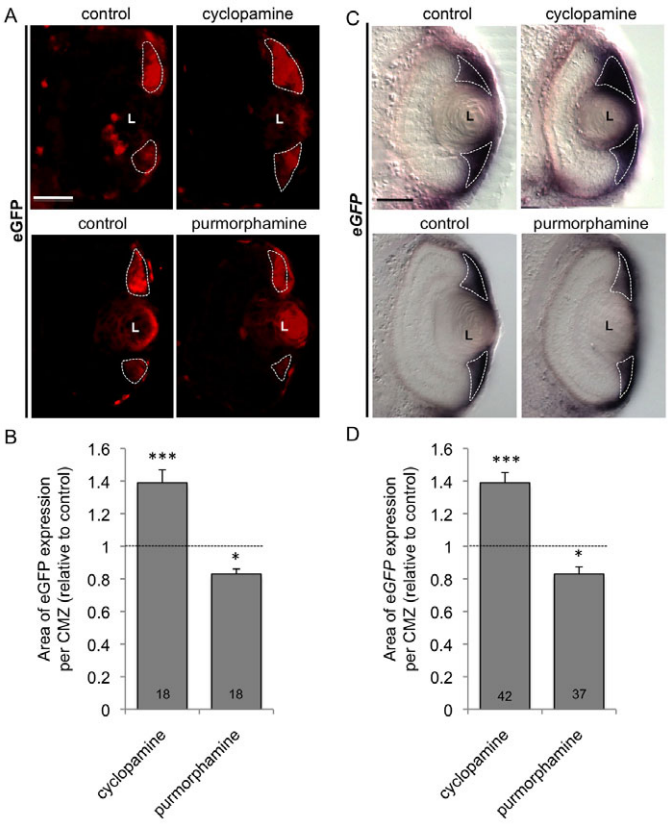

Fig. 7. Hedgehog signalling inhibits Wnt activity. (**A-D**) Immunofluorescence (A,B) or in situ hybridisation (C,D) analyses of *eGFP* expression in stage 40 retinas from Wnt-responsive transgenic animals following a 24-hour treatment with either cyclopamine or purmorphamine. (B,D) Quantification of *eGFP* staining area within the CMZ (delineated by dotted lines). Hoechst staining (for immunolabelling) and Nomarski (for in situ hybridisation) were used to delineate the CMZ in order to exclude RPE *eGFP* labelling from the quantification. The total number of analysed sections per condition is indicated in each bar. **P*<0.05, ****P*<0.001 (Student's *t*-test). Mean ± s.e.m. L, lens. Scale bars: 40 µm.

contains GLI binding sites in its promoter region (Katoh and Katoh, 2006) and has been shown to be regulated by Hedgehog in gastric cancer cells (He et al., 2006). In addition, *Sfrp-1* expression was shown to be enhanced by Hedgehog activation in the developing spinal cord (Domanitskaya et al., 2010). These features make *Sfrp-1* a prime candidate as a potential downstream target of the Hedgehog pathway in the post-embryonic retina. Consistent with this hypothesis, we found that *Sfrp-1* was highly expressed in the periocular mesenchyme, a tissue that lines Ihh- and Dhh-producing cells of the RPE (Fig. 8A) and exhibits Hedgehog signalling activity as inferred by *Ptc1* and *Gli1* expression (Fig. 3D,E and Fig. 5C). Cyclopamine exposure virtually abolished *Sfrp-1* staining, whereas purmorphamine treatment resulted in a marked enhancement of the signal in this region and revealed expression in cells adjacent to the CMZ (peripheral RPE, presumptive cornea and lens epithelium) (Fig. 8A). This upregulation could be observed by qPCR as little as 8 hours following purmorphamine application (Fig. 8B). These data strongly suggest that Hedgehog signalling regulates *Sfrp-1* expression in the mature retina.

As SFRP-1 is known to establish intricate and multiple interactions with the Wnt pathway (Bovolenta et al., 2008), we tested whether it could inhibit Wnt activity in the CMZ. We found that *eGFP* expression was significantly reduced in the retina of Wnt-responsive transgenic tadpoles exposed for 24 hours to SFRP-1 soluble protein (Fig. 8C,D), whereas it was increased upon morpholino-mediated *Sfrp-1* knockdown (Fig. 8E,F). These data are consistent with SFRP-1 acting as a Wnt signalling repressor in this CMZ context.

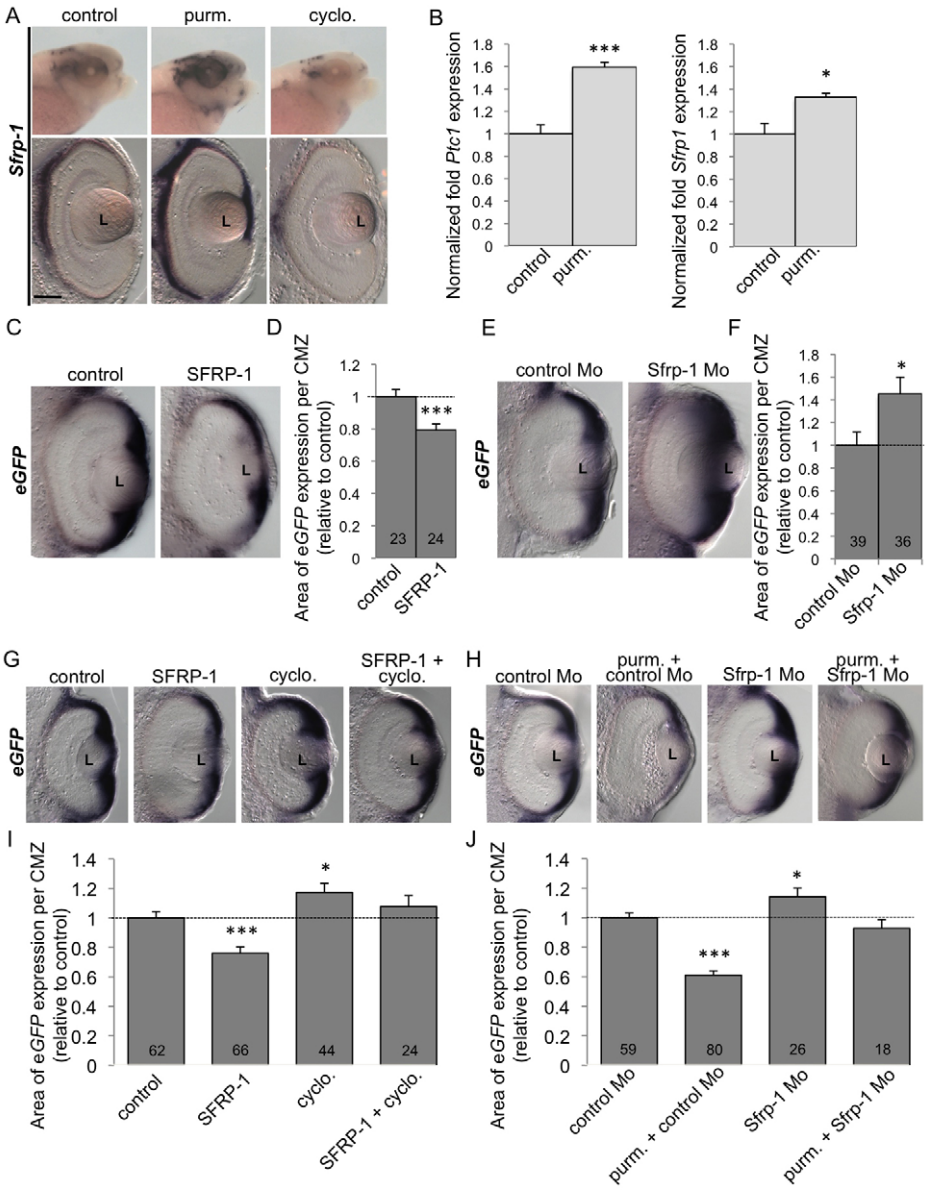

Fig. 8. The Hedgehog pathway negatively regulates Wnt activity through the transcriptional activation of *Sfrp-1*. (**A**) In situ hybridisation analysis of *Sfrp-1* expression on stage 41 retinal sections following a 24-hour treatment with purmorphamine (purm.) or cyclopamine (cyclo.). (**B**) qPCR analysis of *Ptc1* (as a control for purmorphamine activity) and *Sfrp-1* expression in the head of stage 38 sibling tadpoles following 8 hours of purmorphamine exposure. (**C-J**) In situ hybridisation analysis of *eGFP* expression in stage 40 retinas from Wnt-responsive transgenic animals exposed to SRFP-1 protein for 24 hours (C,D,G) or injected with *Sfrp-1* Mo (E,F,H). (G-J) Tadpoles were additionally treated for 24 hours with cyclopamine (G,I) or purmorphamine (H,J). (D,F,I,J) Quantification of *eGFP* staining area per CMZ in each condition. The total number of analysed sections per condition is indicated in each bar. **P*<0.05, ****P*<0.001 (Student's *t*-test). Mean ± s.e.m. L, lens. Scale bar: 40 μm.

Finally, to evaluate whether Hedgehog-dependent downregulation of Wnt activity could be mediated by *Sfrp-1*, we performed rescue experiments in Wnt-responsive transgenic embryos. *eGFP* expression was monitored either in *Sfrp-1* morphant tadpoles treated with purmorphamine or following concomitant exposure to SFRP-1 protein and cyclopamine (Fig. 8G-J). In both cases, eGFP expression was restored to a level similar to that observed in control embryos. We therefore propose that SFRP-1 serves as the molecular link that mediates the negative impact of the Hedgehog pathway on Wnt activity within the post-embryonic retina.

The Wnt/β-catenin pathway downregulates Hedgehog activity in the CMZ through *Gli3* transcriptional regulation

Gli3 is known as a transcriptional repressor of Hedgehog signalling in the absence of ligand stimulation (Jacob and Briscoe, 2003). As it is regulated by Wnt activity in the developing neural tube (Alvarez-Medina et al., 2008; Yu et al., 2008), we examined whether this might also be the case within the CMZ. Indeed, BIO- or LiCl-treated retinas exhibited a significant increase in *Gli3* expression, as assessed by in situ hybridisation or qPCR, whereas IWR-1 exposure led to the opposite phenotype (Fig. 9A-C, supplementary material Fig. S8). This suggests that Gli3 represents a key downstream effector of the Wnt pathway that might account for its negative impact on Hedgehog activity. Consistent with this hypothesis, we found that morpholino-mediated *Gli3* knockdown could rescue the decreased *Ptc1* expression observed in BIO-treated tadpoles (Fig. 9D). We therefore conclude that Wnt-dependent downregulation of Hedgehog activity is mediated by *Gli3* transcriptional regulation.

DISCUSSION

Our study provides new insights into the regulatory network underlying the finely tuned balance between proliferation and differentiation in a post-embryonic neurogenic niche. We discovered unexpected opposed and counterbalancing functions of Wnt and Hedgehog pathways in the tadpole retina that modulate neural stem/progenitor cell proliferation levels. This study also revealed that Hedgehog and Wnt morphogens are expressed in

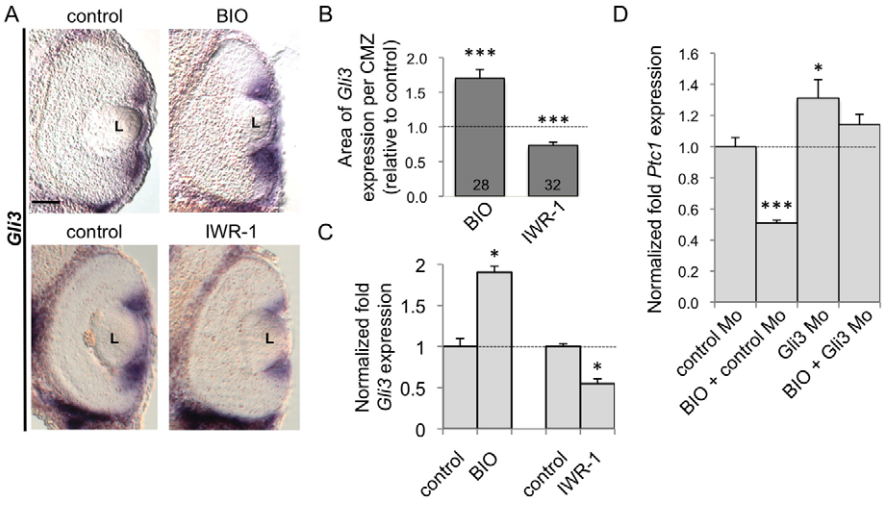

Fig. 9. The Wnt pathway negatively regulates Hedgehog activity through the transcriptional activation of *Gli3*. (**A**,**B**) In situ hybridisation analysis of *Gli3* expression (A) on stage 38 retinal sections 24 hours following BIO or IWR-1 treatment. (B) Quantification of *Gli3* staining area per CMZ. The total number of analysed sections per condition is indicated in each bar. (**C**) qPCR analysis of retinal *Gli3* expression following 24-hour BIO or IWR-1 treatment. (**D**) qPCR analysis of retinal *Ptc1* expression following 24-hour BIO treatment on *Gli3* Mo-injected tadpoles. **P*<0.05, ****P*<0.001 (Student's *t*-test). Mean ± s.e.m. L, lens. Scale bar: 40 μm.

mutually exclusive retinal territories and reciprocally regulate each other's activity within the CMZ. Finally, we showed that this mutual inhibition is achieved by crosstalk involving the transcriptional regulation of *Sfrp-1* and *Gli3*. We propose that an intricate antagonistic interplay of Wnt and Hedgehog pathways tightly regulates the proliferation in the post-embryonic retina (Fig. 10).

A functional antagonism of Wnt and Hedgehog pathways has been described in several developmental processes in both vertebrate and invertebrate species in the context of tissue patterning and cell fate determination (Ahn et al., 2010; Danesin et al., 2009; Glise et al., 2002; Tang et al., 2010; Ulloa and Marti, 2010). Their relationship is however highly dependent on cell context. For instance, they either synergise or exert opposite effects in various aspects of endochondral skeletal development (Mak et al., 2006). Similarly, their interaction during neural development is far from straightforward. Hedgehog is indeed required upstream of the Wnt pathway to promote cell cycle progression in the neural tube (Alvarez-Medina et al., 2009), whereas it must be inhibited by Wnt signalling to allow midbrain progenitor proliferation (Joksimovic et al., 2009). Regarding adult neurogenesis, both pathways are thought to share a mitogenic influence on stem/progenitor cells (reviewed by Mu et al., 2010), suggesting a cooperative mode of action. Strikingly, however, we found in the present study that they instead trigger opposite and counterbalancing proliferative responses within the post-embryonic retina. Based on our lipofection experiments and previous data (Agathocleous et al., 2009; Denayer et al., 2008; Locker et al., 2006), we propose that the Wnt and Hedgehog pathways functionally counteract each other through opposed effects on cell cycle exit. Our study thus highlights for the first time an antagonistic interplay of the two pathways in the control of post-embryonic neural stem/progenitor cell proliferation. Interestingly, opposite influences of Wnt and Hedgehog have recently been described to control colonic epithelial cell renewal in the mammalian intestinal crypt (van den Brink et al., 2004; van Dop et al., 2009). This highlights a striking conservation of their interactions in ontologically unrelated adult stem cell niches.

The mutually exclusive expression patterns of Hedgehog and Wnt ligand genes in the mature retina are highly reminiscent of the situation along the dorsoventral axis of the spinal cord (Ulloa and Marti, 2010). It is thus tempting to imagine the existence of opposing gradients of Wnt and Hedgehog activities within the CMZ. Notably, Wnt signalling activity is not found throughout the whole CMZ but is restricted to its most peripheral half, at or in the immediate vicinity of Wnt ligand-producing cells. It is thus likely that Wnt proteins act locally to mainly influence retinal stem cell and early progenitor behaviour. By contrast, the more central location of Hedgehog ligand production sites suggests that they primarily impact on older progenitors, i.e. cells that are closer to cell cycle exit. Setting up a Hedgehog-responsive transgenic line would help in visualising the precise territory of Hedgehog activity within the CMZ and would be useful to validate this model. Besides, several studies have reported that the magnitude and the duration of Hedgehog signalling input can elicit different proliferative responses (Dessaud et al., 2010; Joksimovic et al., 2009; Ribes et al., 2010). Wnt/Hedgehog interaction modalities might thus vary along the timecourse of neurogenesis within the CMZ and thus differentially affect distinct cellular populations. Consequently, addressing these issues will be pivotal to further understand how these pathways dynamically coordinate post-embryonic neurogenesis in the retina.

We not only found antagonistic functions of the Wnt and Hedgehog pathways in terms of CMZ cell behaviour, but also revealed that they restrain each other's activity and we propose mechanisms underlying this crosstalk. Our results point to the *Sfrp-1* tumour suppressor gene as a key downstream target of the Hedgehog signalling that accounts for Wnt activity attenuation within the CMZ. This interaction is consistent with data from the intestinal crypt, where it was proposed, based on the expression patterns of *Ihh*, *Sfrp-1* and *Wnt6*, that Hedgehog-dependent *Sfrp-1* regulation could help to confine canonical Wnt signalling within stem and progenitor cells (Katoh and Katoh, 2006). For the first time, we formally demonstrate such a scenario in vivo by showing that (1) *Sfrp-1* expression indeed requires Hedgehog signalling, (2) SFRP-1 acts as a Wnt inhibitor in the CMZ and (3) it is necessary for Hedgehog-dependent downregulation of Wnt signalling. Conversely, how does the Wnt pathway counteract Hedgehog activity? As previously observed in the developing chick spinal cord (Alvarez-Medina et al., 2008; Yu et al., 2008), we propose that this occurs through the activation of *Gli3* transcription, as *Gli3* expression is required for the Wnt-dependent negative regulation of Hedgehog signalling. Whether *Sfrp-1* and *Gli3* regulation is sufficient to account for the observed Wnt/Hedgehog reciprocal inhibition remains to be investigated. Indeed, coordination between the two pathways might be more complicated, with additional

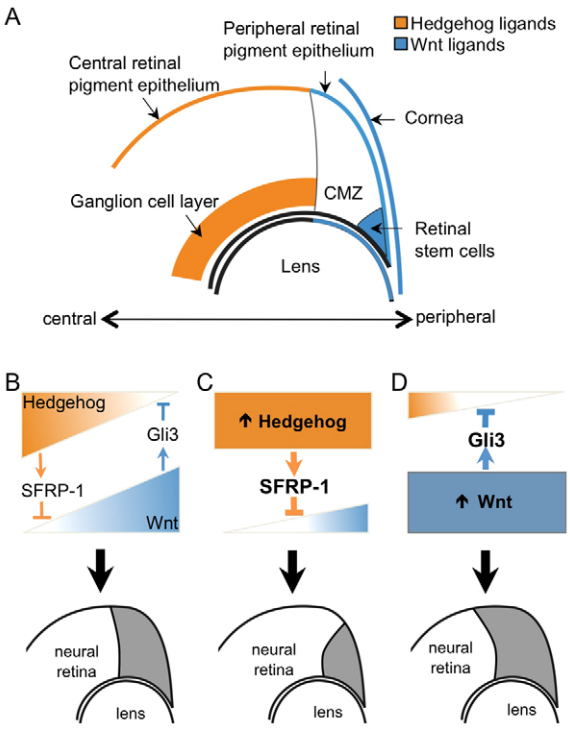

Fig. 10. Model of Wnt and Hedgehog interplay in the post-embryonic retina. (**A**) Schematic highlighting the mutually exclusive expression domains of Wnt and Hedgehog ligands along the central to peripheral axis of the post-embryonic retina. (**B-D**) Illustration of the activities of Wnt and Hedgehog pathways in the retinal neurogenic niche and of the proposed crosstalk underlying their mutual negative regulation. Shown are the hypothetical physiological situation (B), and the synopsis of our Hedgehog (C) or Wnt (D) activation experiments. Their opposed impacts on stem/progenitor cell proliferation are represented by changes in the CMZ proliferative cell population (grey) in the drawings beneath.

players at work, such as Sufu, which antagonises Hedgehog signalling in the retina (Cwinn et al., 2011) and has recently been shown to be involved in Hedgehog and Wnt crosstalk in the early *Xenopus* embryo (Min et al., 2011).

As a whole, our study highlights that stem/progenitor cell proliferation within the post-embryonic retina relies on a balance between opposed Wnt and Hedgehog influences (Fig. 10). This might be of direct relevance for setting up stem cell-based strategies to treat neurodegenerative eye diseases. Unlike in mammals, retinal regeneration in adult anuran amphibians occurs at least partly through CMZ stem cell recruitment (reviewed by Locker et al., 2010). It will thus be valuable to elucidate how the Wnt/Hedgehog balance behaves in the context of retinal injury and how it contributes to retinal repair.

Acknowledgements
We thank S. Sokol, S. Ekker, S. Ohnuma, A. Ruiz i Altaba, K. Takeshima, T. Pieler, P. A. Krieg, R. Moon, A. H. Monsoro-Burq, F. Cremisi and J. C. Saari for providing cDNAs or antibodies; P. Bovolenta for supplying SFRP-1 protein; B. Durand for *Gli3* morpholinos; M. Agathocleous for critical reading of the manuscript; M. Amato, V. Agrawal, J. Hamdache and A. Touzot for help with experiments; and C. de Meideros for animal care.

Funding
This research was supported by grants to M.P. from l'Agence Nationale de la Recherche (ANR), Centre National de la Recherche Scientifique (CNRS), Université Paris-Sud, Retina France, Association pour la Recherche sur le Cancer (ARC), Institut Fédératif de Recherche NeuroSud Paris (IFR144), and to K.V. from the Fonds Wetenschappelijk Onderzoek (FWO), the Belgian Federation against Cancer and the 'Geconcerteerde Onderzoeksacties of Ghent University'. C.B. is an ANR and Region Ile de France Fellow.

Competing interests statement
The authors declare no competing financial interests.

Supplementary material
Supplementary material available online at
http://dev.biologists.org/lookup/suppl/doi:10.1242/dev.079582/-/DC1

References

Adachi, K., Mirzadeh, Z., Sakaguchi, M., Yamashita, T., Nikolcheva, T., Gotoh, Y., Peltz, G., Gong, L., Kawase, T., Alvarez-Buylla, A. et al. (2007). Beta-catenin signalling promotes proliferation of progenitor cells in the adult mouse subventricular zone. *Stem Cells* **25**, 2827-2836.
Agathocleous, M., Locker, M., Harris, W. A. and Perron, M. (2007). A general role of hedgehog in the regulation of proliferation. *Cell Cycle* **6**, 156-159.
Agathocleous, M., Iordanova, I., Willardsen, M. I., Xue, X. Y., Vetter, M. L., Harris, W. A. and Moore, K. B. (2009). A directional Wnt/beta-catenin-Sox2-proneural pathway regulates the transition from proliferation to differentiation in the Xenopus retina. *Development* **136**, 3289-3299.
Ahn, S. and Joyner, A. L. (2005). In vivo analysis of quiescent adult neural stem cells responding to Sonic hedgehog. *Nature* **437**, 894-897.
Ahn, Y., Sanderson, B. W., Klein, O. D. and Krumlauf, R. (2010). Inhibition of Wnt signalling by Wise (Sostdc1) and negative feedback from Shh controls tooth number and patterning. *Development* **137**, 3221-3231.
Alvarez-Medina, R., Cayuso, J., Okubo, T., Takada, S. and Marti, E. (2008). Wnt canonical pathway restricts graded Shh/Gli patterning activity through the regulation of Gli3 expression. *Development* **135**, 237-247.
Alvarez-Medina, R., Le Dreau, G., Ros, M. and Marti, E. (2009). Hedgehog activation is required upstream of Wnt signalling to control neural progenitor proliferation. *Development* **136**, 3301-3309.
Balordi, F. and Fishell, G. (2007). Hedgehog signalling in the subventricular zone is required for both the maintenance of stem cells and the migration of newborn neurons. *J. Neurosci.* **27**, 5936-5947.
Bovolenta, P., Esteve, P., Ruiz, J. M., Cisneros, E. and Lopez-Rios, J. (2008). Beyond Wnt inhibition: new functions of secreted Frizzled-related proteins in development and disease. *J. Cell Sci.* **121**, 737-746.
Centanin, L., Hoeckendorf, B. and Wittbrodt, J. (2011). Fate restriction and multipotency in retinal stem cells. *Cell Stem Cell* **9**, 553-562.
Cerveny, K. L., Varga, M. and Wilson, S. W. (2011). Continued growth and circuit building in the anamniote visual system. *Dev. Neurobiol.* **72**, 328-345.
Chen, B., Dodge, M. E., Tang, W., Lu, J., Ma, Z., Fan, C. W., Wei, S., Hao, W., Kilgore, J., Williams, N. S. et al. (2009). Small molecule-mediated disruption of Wnt-dependent signalling in tissue regeneration and cancer. *Nat. Chem. Biol.* **5**, 100-107.
Cwinn, M. A., Mazerolle, C., McNeill, B., Ringuette, R., Thurig, S., Hui, C. C. and Wallace, V. A. (2011). Suppressor of fused is required to maintain the multipotency of neural progenitor cells in the retina. *J. Neurosci.* **31**, 5169-5180.
Dakubo, G. D., Mazerolle, C., Furimsky, M., Yu, C., St-Jacques, B., McMahon, A. P. and Wallace, V. A. (2008). Indian hedgehog signaling from endothelial cells is required for sclera and retinal pigment epithelium development in the mouse eye. *Dev. Biol.* **320**, 242-255.
Danesin, C., Peres, J. N., Johansson, M., Snowden, V., Cording, A., Papalopulu, N. and Houart, C. (2009). Integration of telencephalic Wnt and hedgehog signalling center activities by Foxg1. *Dev. Cell* **16**, 576-587.
Daniels, M., Dhokia, V., Richard-Parpaillon, L. and Ohnuma, S. (2004). Identification of Xenopus cyclin-dependent kinase inhibitors, p16Xic2 and p17Xic3. *Gene* **342**, 41-47.
de Croze, N., Maczkowiak, F. and Monsoro-Burq, A. H. (2011). Reiterative AP2a activity controls sequential steps in the neural crest gene regulatory network. *Proc. Natl. Acad. Sci. USA* **108**, 155-160.
Decembrini, S., Andreazzoli, M., Vignali, R., Barsacchi, G. and Cremisi, F. (2006). Timing the generation of distinct retinal cells by homeobox proteins. *PLoS Biol.* **4**, e272.
Denayer, T., Locker, M., Borday, C., Deroo, T., Janssens, S., Hecht, A., van Roy, F., Perron, M. and Vleminckx, K. (2008). Canonical Wnt signalling controls proliferation of retinal stem/progenitor cells in postembryonic Xenopus eyes. *Stem Cells* **26**, 2063-2074.
Dessaud, E., Ribes, V., Balaskas, N., Yang, L. L., Pierani, A., Kicheva, A., Novitch, B. G., Briscoe, J. and Sasai, N. (2010). Dynamic assignment and maintenance of positional identity in the ventral neural tube by the morphogen sonic hedgehog. *PLoS Biol.* **8**, e1000382.
Domanitskaya, E., Wacker, A., Mauti, O., Baeriswyl, T., Esteve, P., Bovolenta, P. and Stoeckli, E. T. (2010). Sonic hedgehog guides post-crossing commissural

axons both directly and indirectly by regulating Wnt activity. *J. Neurosci.* **30**, 11167-11176.
Ekker, S. C., McGrew, L. L., Lai, C. J., Lee, J. J., von Kessler, D. P., Moon, R. T. and Beachy, P. A. (1995). Distinct expression and shared activities of members of the hedgehog gene family of Xenopus laevis. *Development* **121**, 2337-2347.
Esteve, P., Trousse, F., Rodriguez, J. and Bovolenta, P. (2003). SFRP1 modulates retina cell differentiation through a beta-catenin-independent mechanism. *J. Cell Sci.* **116**, 2471-2481.
Glise, B., Jones, D. L. and Ingham, P. W. (2002). Notch and Wingless modulate the response of cells to Hedgehog signalling in the Drosophila wing. *Dev. Biol.* **248**, 93-106.
Han, Y. G., Spassky, N., Romaguera-Ros, M., Garcia-Verdugo, J. M., Aguilar, A., Schneider-Maunoury, S. and Alvarez-Buylla, A. (2008). Hedgehog signalling and primary cilia are required for the formation of adult neural stem cells. *Nat. Neurosci.* **11**, 277-284.
He, J., Sheng, T., Stelter, A. A., Li, C., Zhang, X., Sinha, M., Luxon, B. A. and Xie, J. (2006). Suppressing Wnt signalling by the hedgehog pathway through sFRP-1. *J. Biol. Chem.* **281**, 35598-35602.
Jacob, J. and Briscoe, J. (2003). Gli proteins and the control of spinal-cord patterning. *EMBO Rep.* **4**, 761-765.
Joksimovic, M., Yun, B. A., Kittappa, R., Anderegg, A. M., Chang, W. W., Taketo, M. M., McKay, R. D. and Awatramani, R. B. (2009). Wnt antagonism of Shh facilitates midbrain floor plate neurogenesis. *Nat. Neurosci.* **12**, 125-131.
Katoh, Y. and Katoh, M. (2006). WNT antagonist, SFRP1, is Hedgehog signalling target. *Int. J. Mol. Med.* **17**, 171-175.
Koebernick, K., Hollemann, T. and Pieler, T. (2003). A restrictive role for Hedgehog signalling during otic specification in Xenopus. *Dev. Biol.* **260**, 325-338.
Kuwabara, T., Hsieh, J., Muotri, A., Yeo, G., Warashina, M., Lie, D. C., Moore, L., Nakashima, K., Asashima, M. and Gage, F. H. (2009). Wnt-mediated activation of NeuroD1 and retro-elements during adult neurogenesis. *Nat. Neurosci.* **12**, 1097-1105.
Lai, K., Kaspar, B. K., Gage, F. H. and Schaffer, D. V. (2003). Sonic hedgehog regulates adult neural progenitor proliferation in vitro and in vivo. *Nat. Neurosci.* **6**, 21-27.
Lie, D. C., Colamarino, S. A., Song, H. J., Desire, L., Mira, H., Consiglio, A., Lein, E. S., Jessberger, S., Lansford, H., Dearie, A. R. et al. (2005). Wnt signalling regulates adult hippocampal neurogenesis. *Nature* **437**, 1370-1375.
Locker, M., Agathocleous, M., Amato, M. A., Parain, K., Harris, W. A. and Perron, M. (2006). Hedgehog signalling and the retina: insights into the mechanisms controlling the proliferative properties of neural precursors. *Genes Dev.* **20**, 3036-3048.
Locker, M., El Yakoubi, W., Mazurier, N., Dullin, J. P. and Perron, M. (2010). A decade of mammalian retinal stem cell research. *Arch. Ital. Biol.* **148**, 59-72.
Machold, R., Hayashi, S., Rutlin, M., Muzumdar, M. D., Nery, S., Corbin, J. G., Gritli-Linde, A., Dellovade, T., Porter, J. A., Rubin, L. L. et al. (2003). Sonic hedgehog is required for progenitor cell maintenance in telencephalic stem cell niches. *Neuron* **39**, 937-950.
Mak, K. K., Chen, M. H., Day, T. F., Chuang, P. T. and Yang, Y. (2006). Wnt/beta-catenin signalling interacts differentially with Ihh signalling in controlling endochondral bone and synovial joint formation. *Development* **133**, 3695-3707.
Meijer, L., Skaltsounis, A. L., Magiatis, P., Polychronopoulos, P., Knockaert, M., Leost, M., Ryan, X. P., Vonica, C. A., Brivanlou, A., Dajani, R. et al. (2003). GSK-3-selective inhibitors derived from Tyrian purple indirubins. *Chem. Biol.* **10**, 1255-1266.
Min, T. H., Kriebel, M., Hou, S. and Pera, E. M. (2011). The dual regulator Sufu integrates Hedgehog and Wnt signals in the early Xenopus embryo. *Dev. Biol.* **358**, 262-276.
Mu, Y., Lee, S. W. and Gage, F. H. (2010). Signalling in adult neurogenesis. *Curr. Opin. Neurobiol.* **20**, 416-423.
Nieuwkoop, P. D. and Faber, J. (1994). *Normal Table of* Xenopus laevis. New York: Garland.
Ohnuma, S., Philpott, A., Wang, K., Holt, C. E. and Harris, W. A. (1999). p27Xic1, a Cdk inhibitor, promotes the determination of glial cells in Xenopus retina. *Cell* **99**, 499-510.
Ohnuma, S., Mann, F., Boy, S., Perron, M. and Harris, W. A. (2002). Lipofection strategy for the study of Xenopus retinal development. *Methods* **28**, 411-419.
Palma, V., Lim, D. A., Dahmane, N., Sanchez, P., Brionne, T. C., Herzberg, C. D., Gitton, Y., Carleton, A., Alvarez-Buylla, A. and Ruiz i Altaba, A. (2005). Sonic hedgehog controls stem cell behavior in the postnatal and adult brain. *Development* **132**, 335-344.
Perron, M., Kanekar, S., Vetter, M. L. and Harris, W. A. (1998). The genetic sequence of retinal development in the ciliary margin of the Xenopus eye. *Dev. Biol.* **199**, 185-200.
Perron, M., Boy, S., Amato, M. A., Viczian, A., Koebernick, K., Pieler, T. and Harris, W. A. (2003). A novel function for Hedgehog signalling in retinal pigment epithelium differentiation. *Development* **130**, 1565-1577.
Po, A., Ferretti, E., Miele, E., De Smaele, E., Paganelli, A., Canettieri, G., Coni, S., Di Marcotullio, L., Biffoni, M., Massimi, L. et al. (2010). Hedgehog controls neural stem cells through p53-independent regulation of Nanog. *EMBO J.* **29**, 2646-2658.
Ribes, V., Balaskas, N., Sasai, N., Cruz, C., Dessaud, E., Cayuso, J., Tozer, S., Yang, L. L., Novitch, B., Marti, E. et al. (2010). Distinct Sonic Hedgehog signalling dynamics specify floor plate and ventral neuronal progenitors in the vertebrate neural tube. *Genes Dev.* **24**, 1186-1200.
Sekkali, B., Tran, H. T., Crabbe, E., De Beule, C., Van Roy, F. and Vleminckx, K. (2008). Chicken beta-globin insulator overcomes variegation of transgenes in Xenopus embryos. *FASEB J.* **22**, 2534-2540.
Tang, M., Villaescusa, J. C., Luo, S. X., Guitarte, C., Lei, S., Miyamoto, Y., Taketo, M. M., Arenas, E. and Huang, E. J. (2010). Interactions of Wnt/beta-catenin signalling and sonic hedgehog regulate the neurogenesis of ventral midbrain dopamine neurons. *J. Neurosci.* **30**, 9280-9291.
Tran, H. T., Sekkali, B., Van Imschoot, G., Janssens, S. and Vleminckx, K. (2010). Wnt/beta-catenin signalling is involved in the induction and maintenance of primitive hematopoiesis in the vertebrate embryo. *Proc. Natl. Acad. Sci. USA* **107**, 16160-16165.
Ulloa, F. and Marti, E. (2010). Wnt won the war: antagonistic role of Wnt over Shh controls dorso-ventral patterning of the vertebrate neural tube. *Dev. Dyn.* **239**, 69-76.
van den Brink, G. R., Bleuming, S. A., Hardwick, J. C., Schepman, B. L., Offerhaus, G. J., Keller, J. J., Nielsen, C., Gaffield, W., van Deventer, S. J., Roberts, D. J. et al. (2004). Indian Hedgehog is an antagonist of Wnt signalling in colonic epithelial cell differentiation. *Nat. Genet.* **36**, 277-282.
van Dop, W. A., Uhmann, A., Wijgerde, M., Sleddens-Linkels, E., Heijmans, J., Offerhaus, G. J., van den Bergh Weerman, M. A., Boeckxstaens, G. E., Hommes, D. W., Hardwick, J. C. et al. (2009). Depletion of the colonic epithelial precursor cell compartment upon conditional activation of the hedgehog pathway. *Gastroenterology* **136**, 2195-2203 e1-7.
Van Raay, T. J., Moore, K. B., Iordanova, I., Steele, M., Jamrich, M., Harris, W. A. and Vetter, M. L. (2005). Frizzled 5 signalling governs the neural potential of progenitors in the developing Xenopus retina. *Neuron* **46**, 23-36.
Wetts, R., Serbedzija, G. N. and Fraser, S. E. (1989). Cell lineage analysis reveals multipotent precursors in the ciliary margin of the frog retina. *Dev. Biol.* **136**, 254-263.
Xu, Q., D'Amore, P. A. and Sokol, S. Y. (1998). Functional and biochemical interactions of Wnts with FrzA, a secreted Wnt antagonist. *Development* **125**, 4767-4776.
Yu, W., McDonnell, K., Taketo, M. M. and Bai, C. B. (2008). Wnt signalling determines ventral spinal cord cell fates in a time-dependent manner. *Development* **135**, 3687-3696.

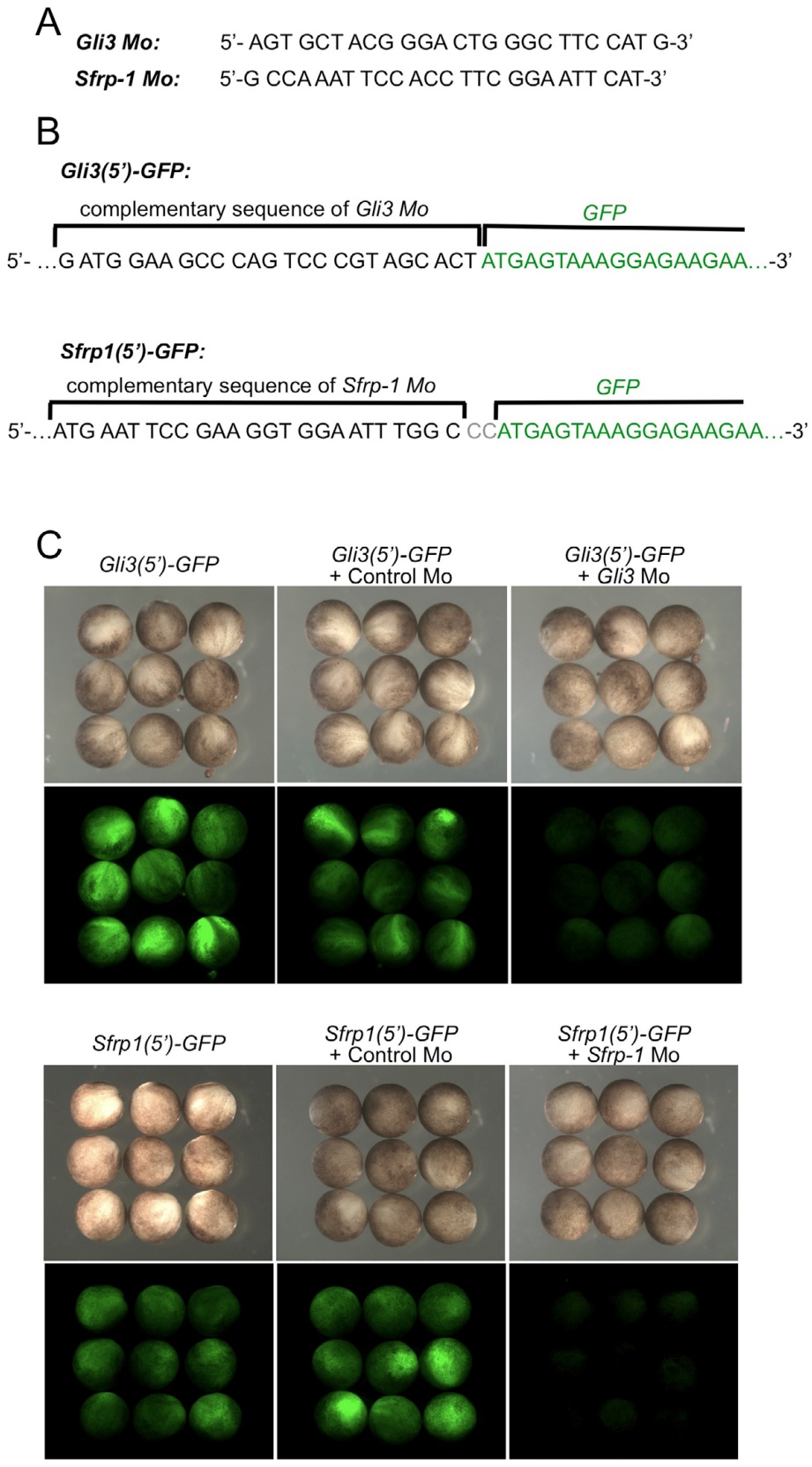

Fig. S1. In vivo validation of *Gli3* and *Sfrp-1* morpholino efficiency. (**A**) *Gli3* and *Sfrp-1* morpholinos (Mo) have been designed to target the ATG region of the corresponding transcripts. (**B**) Schematic representation of the chimeric constructs containing *GFP* fused downstream of *Gli3* or *Sfrp-1* Mo-complementary sequence [*Gli3(5')-GFP* or *Sfrp-1(5')-GFP*]. (**C**) In vivo GFP fluorescence was analysed at stage 19 following co-injection of the indicated Mo and GFP mRNA constructs. *Gli3* and *Sfrp-1* Mo inhibited GFP translation from *Gli3(5')-GFP* and *Sfrp-1(5')-GFP* constructs, respectively, whereas control Mo did not.

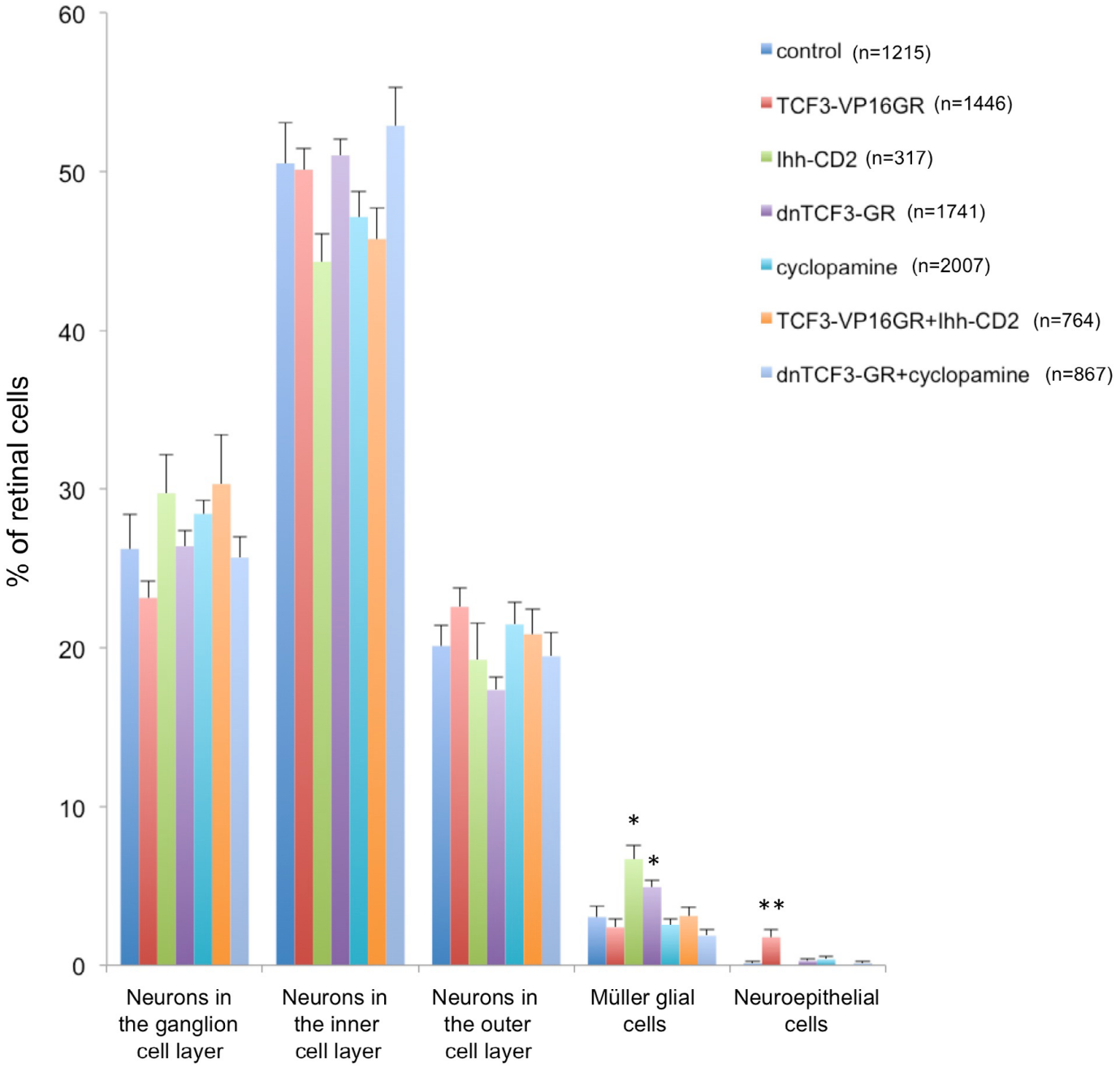

Fig. S2. Clonal analysis of cell type distribution in the retina following interference with Wnt and Hedgehog signalling pathways. Percentage of retinal cells observed in stage 41 retinas following in vivo lipofection with the indicated constructs. Cyclopamine treatment was performed from stage 18 onwards on embryos lipofected with *GFP*. Hedgehog or Wnt signalling perturbation significantly affects the percentage of Müller or neuroepithelial cells (see also Fig. 1). However, as these cells represent very minor cell subpopulations, their variations do not significantly impact on the percentage of neurons (which represent around 95% of total cells). Total number of counted cells is indicated for each condition. *P<0.05, **P<0.01 (Student's t-test).

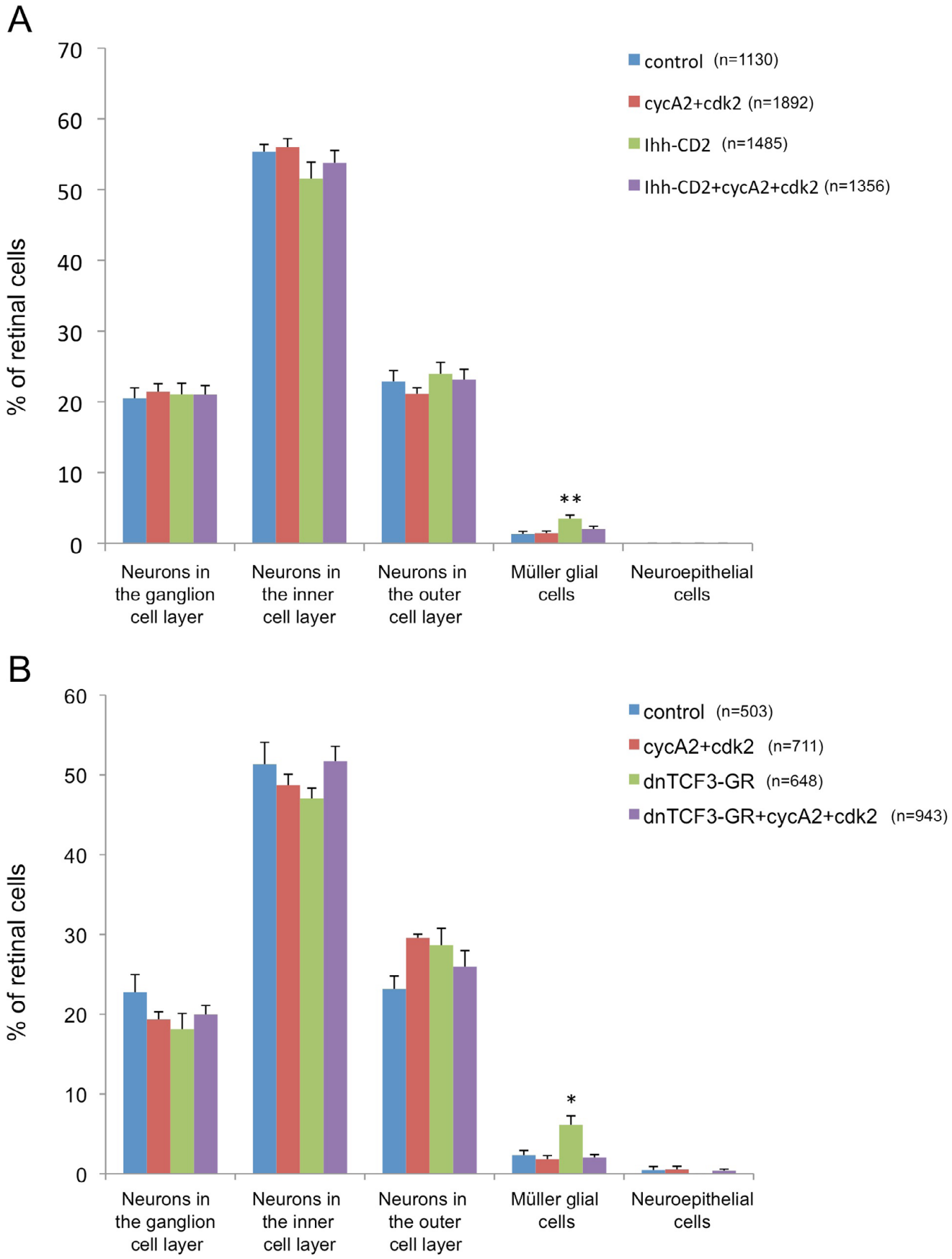

Fig. S3. Co-lipofection of *cyclinA2*/*cdk2* with either *Ihh-CD2* or *dnTCF3-GR* leads to a cell distribution indistinguishable from that observed in a control situation. (**A**,**B**) Percentage of retinal cells observed in stage 41 retinas following in vivo lipofection with the indicated constructs. Total number of counted cells is indicated for each condition. **P*<0.05, ***P*<0.01 (Student's *t*-test).

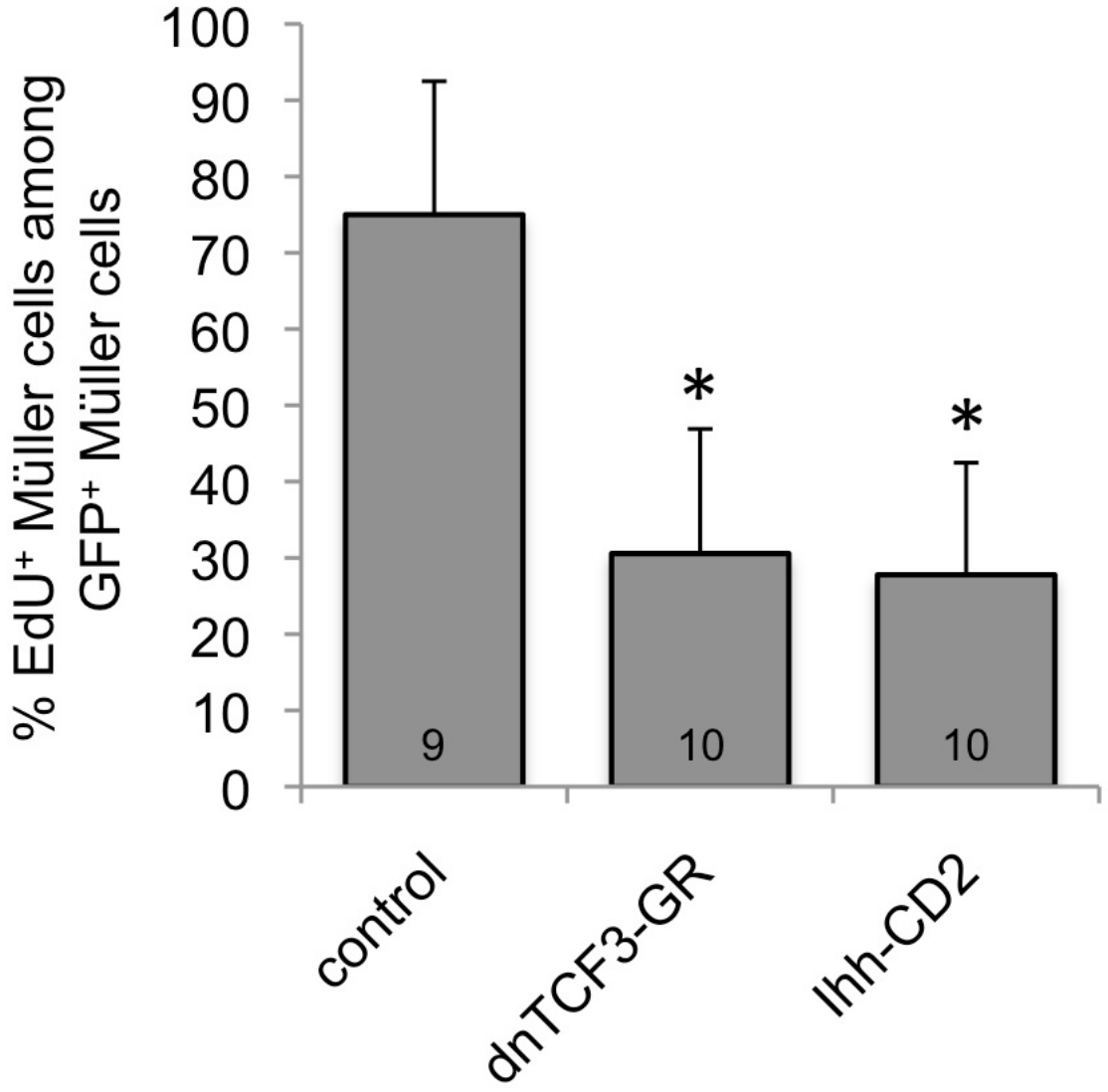

Fig. S4. Hedgehog and Wnt pathways have opposite impacts on cell cycle exit of Müller cells. Birthdating experiments (from stage 32 to stage 41) following in vivo lipofection with the indicated constructs. Transfected Müller cells that have exited the cell cycle before EdU exposure (stage 32) are EdU^- at stage 41, whereas Müller cells that have exited the cell cycle at any time during the EdU incorporation period are EdU^+. Graph represents the percentage of EdU^+ Müller cells among transfected Müller cells. Total number of analysed Müller cells per condition is indicated in each bar. *$P<0.05$ (Student's *t*-test).

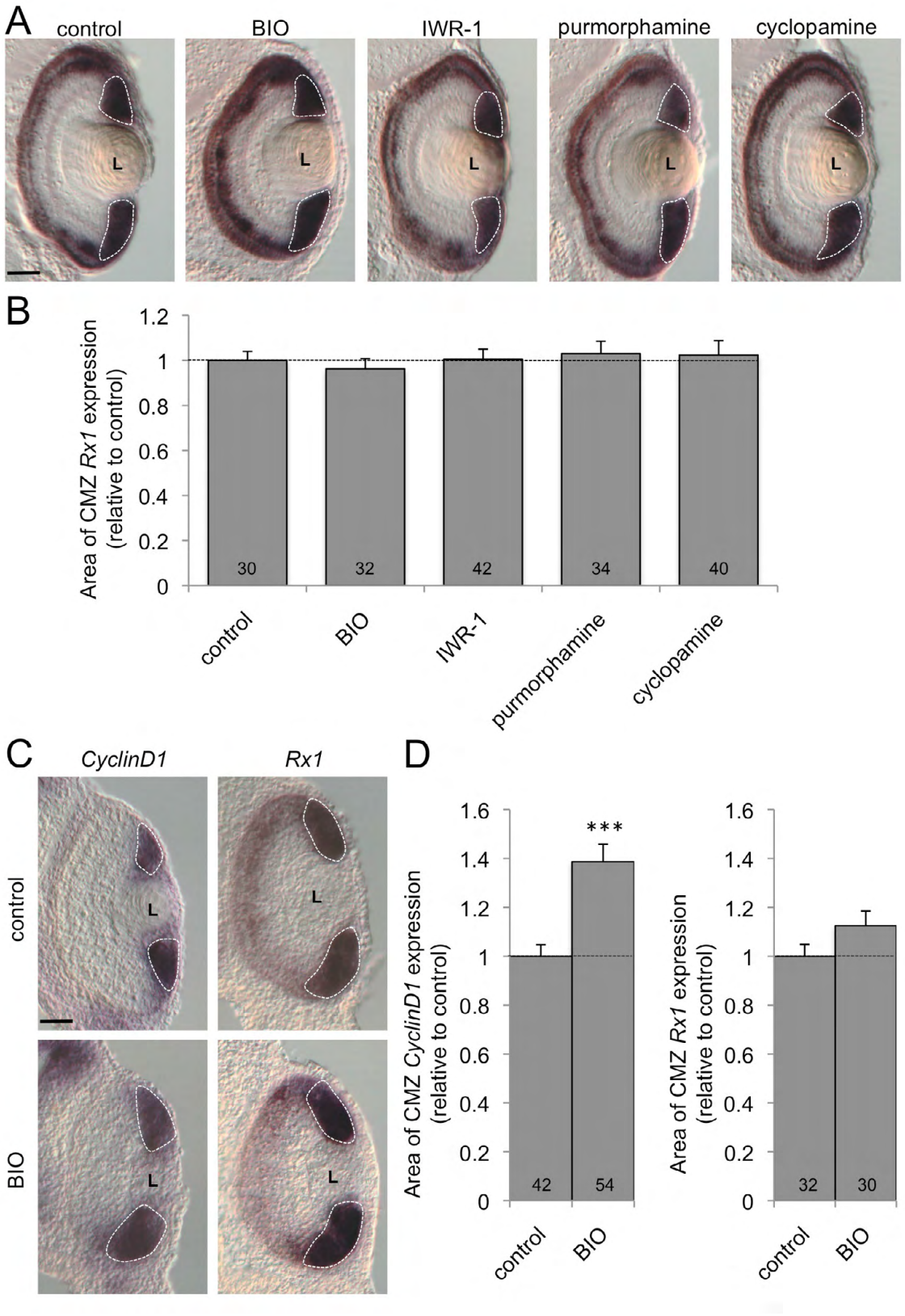

Fig. S5. The overall size of the CMZ is not affected upon pharmacological perturbation of the Wnt or Hedgehog signalling pathway. (**A**,**B**) In situ hybridisation analyses (A) of *Rx1* expression on stage 41 retinal sections 24 hours following BIO, IWR-1, purmorphamine or cyclopamine treatment as indicated. (B) Quantification of *Rx1* staining area per CMZ in each condition. (**C**,**D**) In situ hybridisation analyses (C) of *CyclinD1* or *Rx1* expression on stage 38 retinal sections 24 hours following treatment with BIO. (D) Quantifications of staining area for each transcript. Total number of analysed sections per condition is indicated in each bar. ***P<0.001 (Student's t-test). Labelling in the CMZ is delineated with dotted lines. L, lens. Scale bar: 40 µm.

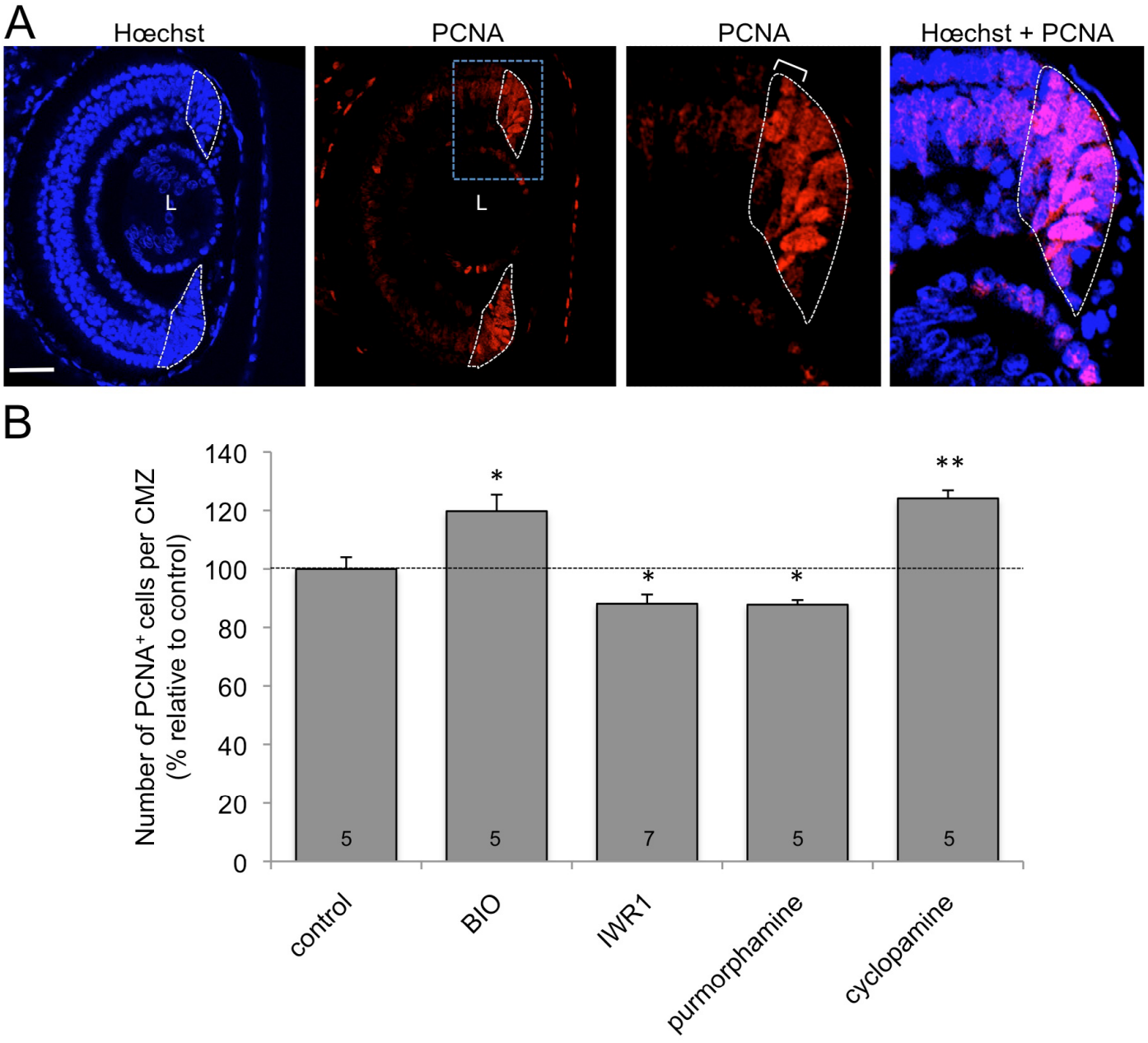

Fig. S6. PCNA immunostaining in the post-embryonic retina following pharmacological perturbation of the Wnt or Hedgehog signalling pathway. PCNA labelling analysis on stage 41 retinal sections 24 hours following treatment with the indicated drugs. (**A**) Typical control retinal section immunostained with anti-PCNA. Pictures on the right show high magnifications of the CMZ (delineated with dotted lines). Note that PCNA labels the whole CMZ, i.e. proliferative cells as expected, but also newly born postmitotic cells in the most central part of the CMZ (bracket). This is likely to be due to the long half-life of the antigen. (**B**) Quantification of PCNA$^+$ cells in the CMZ. Total number of analysed retinas per condition is indicated in each bar. *P<0.05, **P<0.01 (Student's t-test). L, lens. Scale bar: 40 µm.

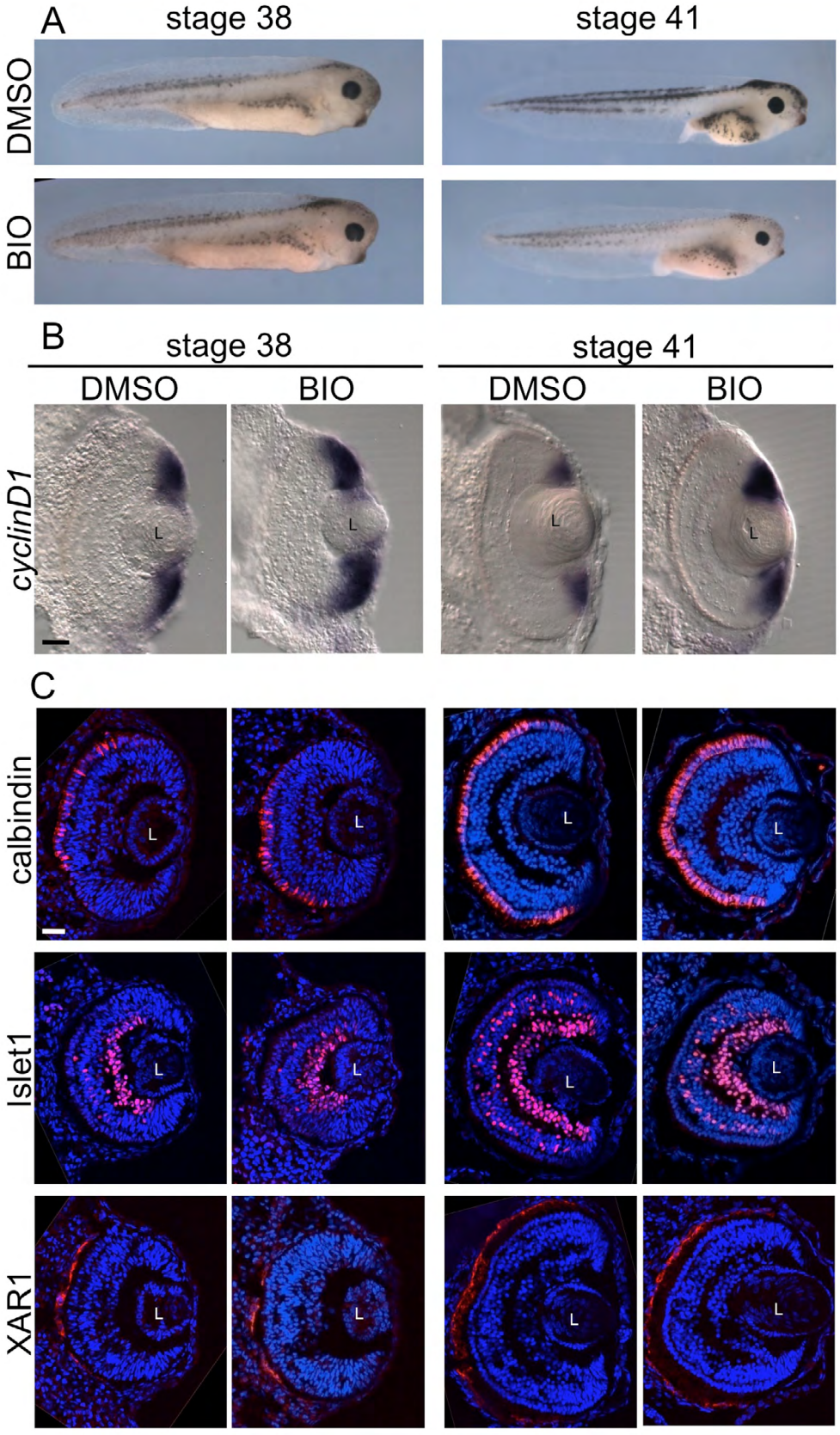

Fig. S7. Twenty-four hours of Wnt pathway activation does not delay development nor does it affect the central retina. (**A**) Tadpoles treated with BIO for 24 hours do not display any developmental delay, as judged by their overall morphology. (**B**) In situ hybridisation analysis of *CyclinD1* expression on retinal sections following a 24-hour BIO treatment, illustrating the effective activation of the Wnt pathway. (**C**) Immunofluorescence analysis of cell type-specific markers on sibling tadpoles. Calbindin is a marker of photoreceptor cells, Islet1 labels ganglion cells and a subtype of bipolar cells and XAR1 stains the RPE. L, lens. Scale bar: 40 µm.

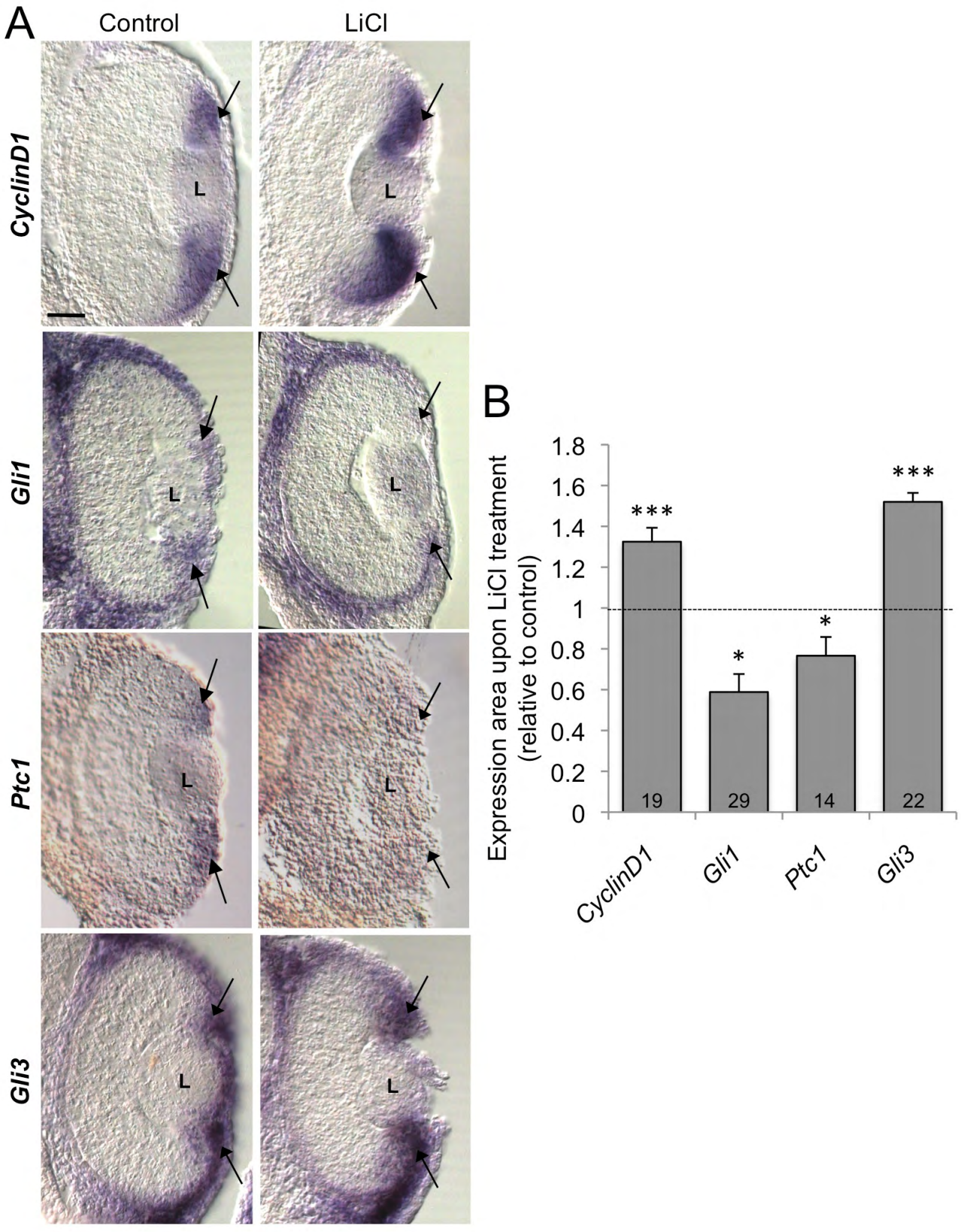

Fig. S8. Wnt pathway activation downregulates the Hedgehog target genes *Gli1* and *Ptc1* but increases *Gli3* expression. (**A**,**B**) In situ hybridisation analyses (A) of *CyclinD1*, *Gli1*, *Ptc1* or *Gli3* expression on stage 38 retinal sections 24 hours following LiCl treatment. Arrows indicate CMZ labelling. (B) Quantification of staining area for each gene. Compared with controls, LiCl-treated embryos exhibit decreased *Gli1* and *Ptc1* staining, whereas *Gli3* expression is enhanced. Total number of analysed sections per condition is indicated in each bar. **P*<0.05, ****P*<0.001 (Student's *t*-test). L, lens. Scale bar: 40 µm.

Table S1. PCR primer sequences

***Xenopus laevis* qPCR primers**		
Gene	**Forward primer**	**Reverse primer**
Gli3	GGCCCCCACCAACACCACTG	CCGTGGGACATTGACCGAAGGA
Patched1	CAGCTGCCCAGCCGAGGGTA	GGGCGAAATTGGCATCGCAGTA
ODC	GCTTCTGGAGCGGGCAAAGGA	CCAAGCTCAGCCCCCATGTCA
RPL8	CCACGTGTCCGTGGTGTGGCTA	GCGCAGACGACCAGTACGACGA
Sfrp1	CAGTGAGACAATGGCGGAGGTGAA	GGGGCGAAGAGAGAGCACAGGA
***Xenopus tropicalis* qPCR primers**		
Gene	**Forward primer**	**Reverse primer**
Patched1	CAGCTGCCCAGCCGAGGGTA	TCCTGGTCAGGCGGCGCTACTA
ODC	CATGGCATTCTCCCTGAAGTACCAGAA	GGACAGATGGTAGGGGCAAGCTCA
RPL8	CGCCACCGTTATCTCCCACAATC	CCACCAGCAACAACCCCAACA